Electronic Supplementary Material (ESI) for ChemComm.

Electronic Supporting Information (SI)

Catalytically Active Nanorotor Reversibly Self-Assembled by Chemical Signaling within an Eight-Component Network

Abir Goswami, Susnata Pramanik, Michael Schmittel*

Center of Micro- and Nanochemistry and Engineering, Organische Chemie I, Universität Siegen, Adolf-Reichwein-Str. 2, D-57068 Siegen, Germany.

E-mail: schmittel@chemie.uni-siegen.de

Fax: (+49) 271-740-3270

Table of Contents

1. Synthesis

1.1 General Remarks

All commercial reagents were used without further purification. Solvents were dried with the appropriate desiccants and distilled prior to use. Bruker Avance (400 MHz) and Varian (600 MHz) spectrometers were used to measure ^{1}H and ^{13}C NMR spectra employing a deuterated solvent as the lock and residual protiated solvent as internal reference ($CDCl_3$: δ_H 7.26 ppm, δ_C 77.0 ppm; CD_2Cl_2: δ_H 5.32 ppm, δ_C 53.8 ppm, THF-d_8: δ_H 1.72 ppm, 3.58 ppm, δ_C 25.3 ppm, 67.2 ppm). The following abbreviations were used to describe NMR peak pattern: s = singlet, d = doublet, t = triplet, dd = doublet of doublets, ddd = doublet of doublets of doublets, td = triplet of doublets, br = broad, m = multiplet. The coupling constant values are given in Hertz (Hz) and, wherever possible, assignment of protons is provided. The numbering of different carbons in different molecular skeletons does not necessarily follow IUPAC nomenclature rules; it was exclusively implemented for assigning NMR signals. All electrospray ionization (ESI-MS) spectra were recorded on a Thermo-Quest LCQ deca and the theoretical isotopic distributions of the mass signals were calculated using IsoPro 3.0 software. Melting points of compounds were measured on a BÜCHI 510 instrument and are not corrected. Infrared spectra were recorded on a Varian 1000 FT-IR instrument. Elemental analysis was performed using the EA-3000 CHNS analyzer. UV-vis spectra were recorded on a Cary Win 50 (298 K) spectrometer. Binding constants were determined through UV-vis titrations in combination with a 1:1 binding formula of two ligands or with SPECFIT/32TM global analysis system by Spectrum Software Associates (Marlborough, MA). Column chromatography was performed either on silica gel (60-400 mesh) or neutral alumina (Fluka, 0.05-0.15 mm, Brockmann Activity 1). Merck silica gel (60 F254) or neutral alumina (150 F254) sheets were used for thin layer chromatography (TLC). The multi-component assembly of rotors was performed directly in the NMR tube with CD_2Cl_2 as solvent. Compounds **1**,[1] **6**,[2] **7**,[3] **A**[4] were synthesized according to literature known procedures.

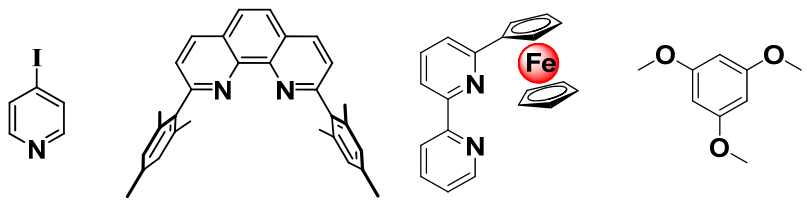

2 **3** **4** **5**

Scheme S1. Compounds **2**-**4** used in the model self-sorting and compound **5** used as internal standard in catalysis.

1.2 Synthesis of stators, rotators and nanoswitches

Zinc(II)-*meso*-5,15-bis-{4-[2-(4-bromo-2,3,5,6-tetramethylphenyl)-9-(2,4,6-trimethylphenyl)-[1,10]phenanthrolinyl-3-ethinyl]phenyl}-10,20-bis-(2,4,6-trimethyl phenyl)porphyrin (S).

In an oven-dried 100 mL sealed tube, a mixture of 2-(2,3,5,6-tetramethyl-4-bromophenyl)3-ethynyl-9-(2,4,6-trimethylphenyl)-1,10-phenanthroline (**6**) (150 mg, 281 µmol) and *meso* 5,15-bis(mesityl)-10,20-bis(4-iodophenyl)porphyrin (**7**) (100 mg, 98.6 µmol) was dissolved in dry benzene (20 mL) and Et_2NH (20 mL). After thorough degassing, $Pd(PPh_3)_4$ (30.0 mg, 26.0 µmol) was added and the

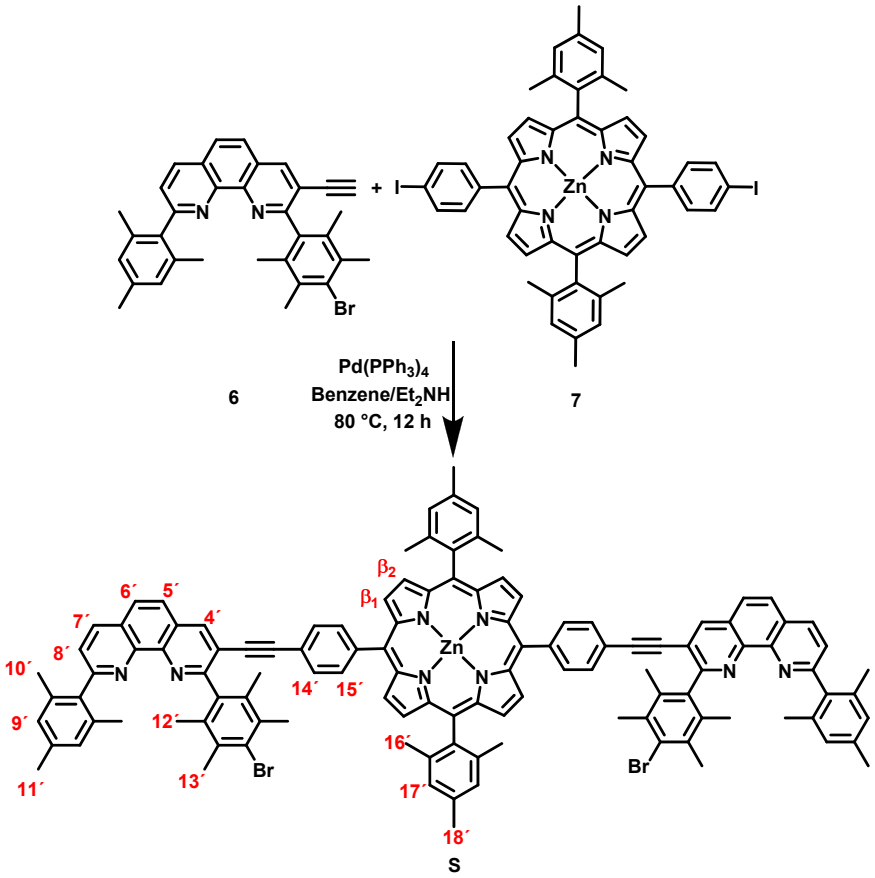

Scheme S2. Synthesis of stator (**S**).

mixture was refluxed at 80 °C for 12 h for completion of the coupling reaction. The reaction mixture was cooled down to room temperature and the solvents were removed. The residue was subjected to column chromatography (silica gel, CH_2Cl_2, R_f = 0.3) to afford 120 mg of ligand **S** as violet solid (65.7 µmol, 67%). **Melting point:** >300 °C; **IR** (KBr)**:** $\tilde{\nu}$ = 3441, 2963, 2914, 2733, 2362, 2201, 1913, 1804, 1701, 1602, 1491, 1442, 1263, 1162, 1093, 994, 846, 802, 765, 722, 573 cm^{-1}; **^{1}H NMR (400 MHz, $CDCl_3$):** δ= 8.85 (d, 4H, ^3J = 4.6 Hz, β_1-H), 8.79 (d, 4H, ^3J = 4.6 Hz, β_2-H), 8.63 (s, 2H, 4′-H), 8.33 (d, ^3J = 8.4 Hz, 2H, 7′-H), 8.17 (d, ^3J = 8.0 Hz, 4H, 15′-H), 7.95 (d, 2H, ^3J = 9.0 Hz, 6′/5′-H), 7.92 (d, ^3J = 9.0 Hz, 2H, 5′/6′-H), 7.61 (d, ^3J = 8.4 Hz, 2H, 8′-H), 7.49 (d, ^3J = 8.0 Hz, 4H, 14′-H), 7.29 (s, 4 H, 17′-H), 6.96 (s, 4 H, 9′-H), 2.64 (s, 6H, 18′-H), 2.53 (s, 12H, 12′-H), 2.33 (s,

6H, 11′-H), 2.16 (s, 12H, 13′-H), 2.13 (s, 12H, 10′-H), 1.83 (s, 12H, 16′-H); **^{13}C NMR (100 MHz $CDCl_3$):** δ = 162.6, 160.7, 150.0, 149.7, 145.9, 144.7, 143.4, 139.2, 139.2, 138.9, 138.5, 137.9, 137.6, 137.5, 136.1, 136.0, 134.5, 133.8, 133.7, 132.1, 131.0, 129.7, 129.3, 128.5, 127.7, 127.7, 127.2, 127.0, 125.7, 125.2, 121.8, 120.2, 119.6, 119.3, 95.7, 87.8, 21.6, 21.5, 21.1, 21.1, 20.5, 18.7; **ESI-MS:** *m/z* (%) = 1825.6 (60) $[M+H]^+$, 913.4 (100) $[M+2H]^{2+}$; **UV-Vis:** λ_{abs} (CH_2Cl_2) = 422, 549, 595 nm; ε_{422} = 2.17 × 10^4 $M^{-1}cm^{-1}$; **Elemental analysis:** ($C_{116}H_{94}Br_2N_8Zn$): calculated: C 76.33; H. 5.19; N. 6.14; found: C 76.32; H. 5.10; N. 5.92.

Spectroscopic data for nanoswitch 1

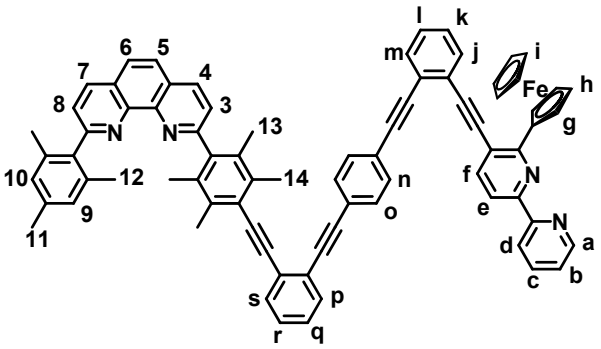

The preparation was executed as described earlier.[1] **Melting point:** 165-168 °C; **IR (KBr)**: $\tilde{\nu}$ = 3052, 2993, 2916, 2862, 2280, 2200, 1950, 1922, 1810, 1697, 1600, 1582, 1540, 1500, 1479, 1436, 1385, 1350, 1265, 1214, 1166, 1139, 1095, 1012, 952, 842, 756, 627, 585 cm^{-1}; **^{1}H NMR (400 MHz, CD_2Cl_2):** δ = 8.68 (ddd, ^3J = 4.8 Hz, ^4J = 1.2 Hz, ^5J = 1.2 Hz, 1H, a-H), 8.54 (dt, ^3J = 8.0 Hz, ^4J = 1.2 Hz, ^5J = 1.2 Hz, 1H, d-H), 8.33 (d, ^3J = 8.0 Hz, 1H, 4-H), 8.32 (d, ^3J = 8.0 Hz, 1H, 7-H), 8.23 (d, ^3J = 8.4 Hz, 1H, e-H), 7.95 (d, ^3J = 8.4 Hz, 1H, f-H), 7.90 (s, 2H, 5-, 6-H), 7.78 (td, ^3J = 8.0 Hz, ^4J = 1.2 Hz, 1H, c-H), 7.70-7.72 (m, 1H, s-H), 7.61-7.67 (m, 3H, j-, m-, p-H), 7.56 (d, ^3J = 8.0 Hz, 1H, 3-H), 7.54 (s, 4H, n-, o-H), 7.52 (d, ^3J = 8.0 Hz, 1H, 8-H), 7.40-7.46 (m, 2H, q-, r-H), 7.33-7.39 (m, 2H, k-, l-H), 7.21 (ddd, ^3J = 8.0 Hz, ^3J = 4.8 Hz, ^4J = 1.2 Hz, 1H, b-H), 6.95 (s, 2H, 9-, 10-H), 5.57 (t, ^3J = 2.0 Hz, 2H, g-H), 4.32 (t, ^3J = 2.0 Hz, 2H, h-H), 4.06 (s, 5H, i-H), 2.56 (s, 6H, 14-H), 2.32 (s, 3H, 11-H), 2.03 (s, 6H, 12-H), 1.91 (s, 6H, 13-H) ppm; **^{13}C NMR (100 MHz, CD_2Cl_2)**: δ = 161.3, 160.5, 159.1, 156.0, 154.6, 149.4, 146.6, 146.6, 142.8, 142.1, 138.4, 137.7, 137.0, 136.7, 136.4, 136.3, 136.0, 132.7, 132.6, 132.4, 132.2, 132.1, 132.1, 132.0, 128.8, 128.8, 128.7, 128.5, 128.1, 127.6, 127.5, 126.7, 126.6, 126.4, 125.9, 125.6, 124.9, 124.9, 124.7, 124.1, 123.7, 123.2, 123.0, 121.4, 117.0, 115.9, 95.8, 95.0, 93.6, 93.5, 93.2, 92.9, 91.0, 90.4, 84.0, 70.3, 70.1, 70.0, 21.2, 20.4, 18.7, 17.7 ppm. **ESI-MS:** *m/z* (%) = 1093.4 (100) [**1**+H]$^+$; **Elemental analysis:** ($C_{77}H_{56}FeN_4$• 0.5CH_3COOEt): Calculated: C, 83.59; H, 5.15; N, 4.94; Found: C, 83.27; H, 5.17; N, 5.00.

Spectroscopic data for rotator R

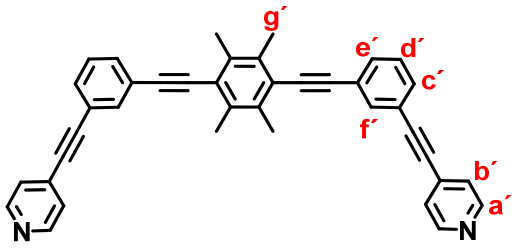

The full synthesis of rotator **R** will be presented in a follow-up publication soon. Below, we provide the full characterization of **R**. **Melting point:** 210-212 °C; **IR (KBr):** $\tilde{\nu}$ = 3050, 2923, 2211, 1593, 1569, 1537, 1489, 1478, 1404, 1375, 1315, 1214, 1090, 1066, 1014, 988, 936, 919, 820, 795, 748, 686, 646, 587, 565, 544, 533, 497 cm^{-1}; **^{1}H NMR (400 MHz, CD_2Cl_2):** δ = 8.61 (d, ^3J = 6.0 Hz, 4H, a´-H), 7.74 (t, ^4J = 1.6 Hz, 2H, f´-H), 7.57 (dt, ^3J = 8.0 Hz, ^4J = 1.6 Hz, 2H, e´/c´-H), 7.52 (dt, ^3J = 8.0 Hz, ^4J = 1.6 Hz, 2H, c´/e´-H), 7.40 (d, ^3J = 6.0 Hz, 4H, b´-H), 7.38 (t, ^3J = 8.0 Hz, 2H, d´-H), 2.51 (s, 12H, g´-H) ppm; **^{13}C NMR (100 MHz, $CDCl_3$):** δ = 149.8, 135.8, 134.4, 131.9, 131.3, 131.1, 128.6, 125.5, 124.3, 123.2, 122.5, 97.1, 93.1, 89.5, 87.2, 18.4 ppm; **ESI-MS:** *m/z* (%) 537.4 (100) $[R + H]^+$; **Elemental analysis:** Calculated: ($C_{40}H_{28}N_2 \bullet H_2O$): C, 86.61; H, 5.45; N, 5.05; Found: C, 86.47; H, 5.06; N, 4.70.

2. Synthesis and characterization of complexes

All solid compounds were placed in an NMR tube and then dissolved in CD_2Cl_2. Subsequently NMR spectra were measured at 298 K. $Zn(OTf)_2$ was added as a standard solution in CD_3CN.

Complex C1 = $[Cu(\mathbf{3})(\mathbf{4})]^+$

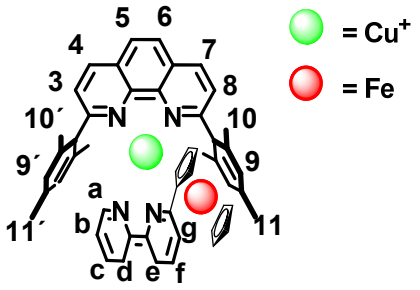

[Cu(3)(4)]$^+$

In an NMR tube, 2,9-dimesityl-[1,10]-phenanthroline (**3**) (0.592 mg, 1.42 µmol), 6-ferrocenyl-2,2´-bipyridine (**4**) (0.483 mg, 1.42 µmol), and $[Cu(CH_3CN)_4]PF_6$ (0.530 mg, 1.42 µmol) were dissolved in 500 µL of CD_2Cl_2. Yield by NMR: quantitative; **^{1}H NMR (400 MHz, CD_2Cl_2):** δ = 8.57 (d, ^3J = 8.8 Hz, 2H, 4-, 7-H), 8.10 (s, 2H, 5-, 6-H), 7.95 (dd, ^3J = 4.8 Hz, ^4J = 1.6 Hz, 1H, a-H), 7.85 (td, ^3J

= 8.0 Hz, ^4J = 1.6 Hz, 1H, c-H), 7.79 (d, ^3J = 8.0 Hz, 1H, d-H), 7.78 (t, ^3J = 8.0 Hz, 1H, f-H), 7.77 (d, ^3J = 8.8 Hz, 2H, 3-, 8-H), 7.65 (d, ^3J = 8.0 Hz, 1H, g-H), 7.33 (d, ^3J = 8.0 Hz, 1H, e-H), 7.27 (ddd, ^3J = 8.0 Hz, ^3J = 4.8 Hz, ^4J = 1.6 Hz, 1H, b-H), 6.40 (s, 2H, 9/9´-H), 6.37 (s, 2H, 9´/9-H), 4.06 (brs, 2H, Fc-H), 3.82 (brs, 5H, Fc-H), 3.44 (brs, 2H, Fc-H), 2.00 (s, 6H, 11+11´-H), 1.82 (s, 6H, 10/10´-H), 1.77 (s, 6H, 10´/10-H) ppm; **ESI-MS:** *m/z* (%) = 819.9 (100) [[Cu(**3**)(**4**)]$^+$].

Complex C2 = [Zn(**3**)(**4**)]$^{2+}$

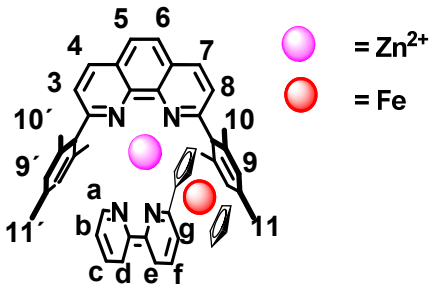

[Zn(3)(4)]$^{2+}$

In an NMR tube **3** (0.662 mg, 1.59 µmol), **4** (0.540 mg, 1.59 µmol) were dissolved in 500 µL of CD_2Cl_2. NMR spectra were measured immediately after addition of $Zn(OTf)_2$ (0.578 mg, 1.59 µmol) as a standard solution in CD_3CN. Yield: quantitative. **^{1}H NMR (400 MHz, CD_2Cl_2):** δ = 9.04 (d, ^3J = 8.8 Hz, 2H, 4-, 7-H), 8.41 (s, 2H, 5-, 6-H), 8.36 (d, ^3J = 4.6 Hz, 1H, a-H), 8.31 (td, ^3J = 8.0 Hz, ^4J = 1.2 Hz, 1H, c-H), 8.25 (dd, ^3J = 8.0 Hz, ^4J = 1.2 Hz, 1H, d-H), 8.19 (t, ^3J = 8.0 Hz, 1H, f-H), 8.12 (dd, ^3J = 8.0 Hz, ^4J = 1.2 Hz, 1H, g-H), 8.08 (d, ^3J = 8.8 Hz, 2H, 3-, 8-H), 8.05 (dd, ^3J = 8.0 Hz, ^4J = 1.2 Hz, 1H, e-H), 7.73 (ddd, ^3J = 8.0 Hz, ^3J = 4.6 Hz, ^4J = 1.2 Hz, 1H, b-H), 6.39 (s, 2H, 9/9´-H), 6.25 (s, 2H, 9´/9-H), 4.05 (brs, 2H, Fc-H), 3.97 (brs, 5H, Fc-H), 3.78 (brs, 2H, Fc-H), 1.91 (s, 6H, 11-, 11´-H), 1.76 (s, 6H, 10/10´-H), 1.70 (s, 6H, 10´/10-H) ppm; **ESI-MS:** *m/z* (%) = 969.6 (100) [[Zn(**3**)(**4**)+OTf$^-$]$^+$].

Complex C3 = [(**S**)•(**R**)]

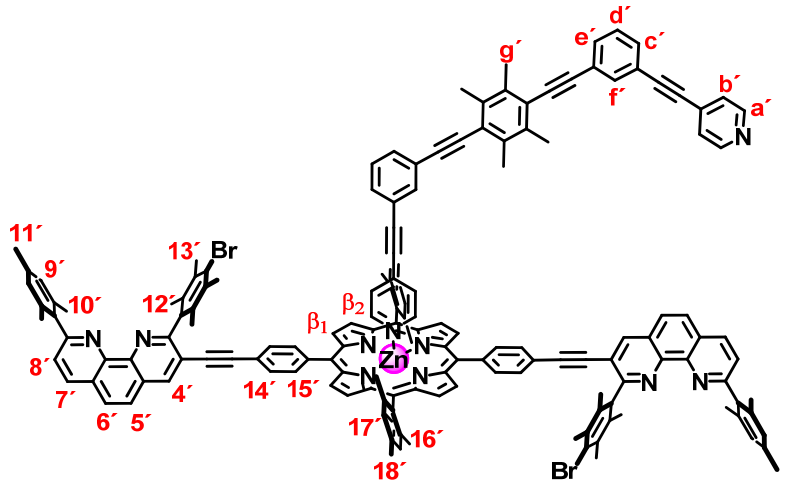

In an NMR tube, stator **S** (1.08 mg, 0.592 µmol) and rotator **R** (0.318 mg, 0.592 µmol) were dissolved in 500 µL of CD_2Cl_2. The NMR spectrum suggested full conversion. **Mp** > 250 °C; **IR (KBr):** $\tilde{\nu}$ = 3027, 2917, 2210, 1596, 1523, 1489, 1458, 1381, 1336, 1263, 1203, 1063, 995, 896, 849, 796, 721, 684, 638, 623, 543 cm^{-1}; **^{1}H NMR (400 MHz, CD_2Cl_2):** 8.79 (d, 4H, ^3J = 4.8 Hz, β_1-H), 8.70 (d, 4H, ^3J = 4.8 Hz, β_2-H), 8.65 (s, 2H, 4′-H), 8.36 (d, ^3J = 8.4 Hz, 2H, 7′-H), 8.14 (d, ^3J = 8.0 Hz, 4H, 15′-H), 7.98 (d, 2H, ^3J = 9.0 Hz, 6′/5′-H), 7.95 (d, ^3J = 9.0 Hz, 2H, 5′/6′-H), 7.59 (d, ^3J = 8.4 Hz, 2H, 8′-H), 7.55 (t, ^4J = 1.6 Hz, 2H, f′-H), 7.50 (d, ^3J = 8.0 Hz, 4H, 14′-H), 7.50 (1H, c′-H merged with 14′-H), 7.34 (dt, ^3J = 7.8 Hz, ^4J = 1.6 Hz, 2H, e′-H), 7.31 (t, ^3J = 7.8 Hz, 2H, d′-H), 7.29 (s, 4H, 17′-H), 6.97 (s, 4H, 9′-H), 6.58 (brs, 4H, b′-H), 5.71 (brs, 4H, a′-H), 2.62 (s, 6H, 18′-H), 2.54 (s, 12H, 12′-H), 2.44 (s, 12H, g′-H), 2.34 (s, 6H, 11′-H), 2.13 (s, 12H, 13′-H), 2.07 (s, 12H, 10′-H), 1.81 (s, 12H, 16′-H); **UV-Vis:** λ_{abs} (CH_2Cl_2) = 426, 553, 599 nm; ε_{426} = 2.11 × 10^4 $M^{-1}cm^{-1}$; **Elemental analysis:** ($C_{156}H_{122}Br_2N_{10}Zn$• $2H_2O$): Calculated: C, 78.14; H, 5.30; N, 5.84. Found: C, 78.22; H, 4.94; N, 5.75.

Complex C4 = $[Cu_2(\mathbf{S})(\mathbf{R})]^{2+}$

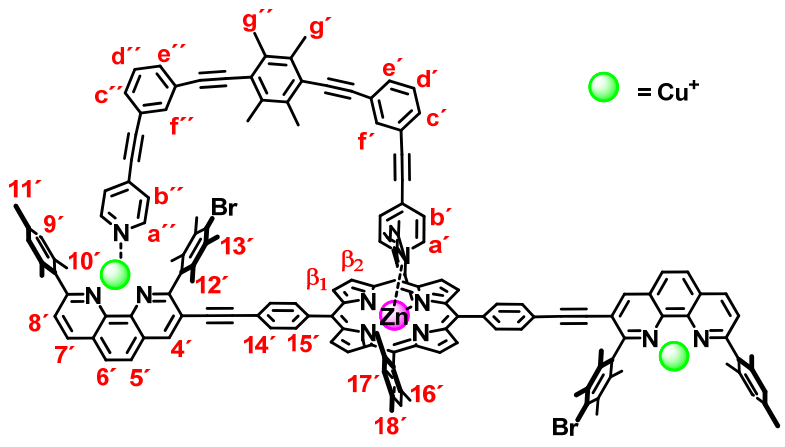

In an NMR tube, $[Cu(CH_3CN)_4]PF_6$ (0.422 mg, 1.13 µmol), stator **S** (1.03 mg, 0.564 µmol), and rotator **R** (0.302 mg, 0.564 µmol) were dissolved in 500 µL of CD_2Cl_2. The NMR spectrum indicated quantitative formation of the nanorotor $[Cu_2(\mathbf{S})(\mathbf{R})]^{2+}$. **Mp** > 250 °C; **IR (KBr):** $\tilde{\nu}$ = 3036, 2919, 2209, 1605, 1491, 1459, 1382, 1336, 1203, 1064, 996, 843, 796, 719, 683, 623, 560 cm^{-1}; **^{1}H NMR (400 MHz, CD_2Cl_2):** 8.95 (s, 2H, 4′-H), 8.80 (d, 4H, ^3J = 4.4 Hz, β_1-H), 8.76 (d, ^3J = 8.4 Hz, 2H, 7′-H), 8.74 (d, 4H, ^3J = 4.4 Hz, β_2-H), 8.26 (d, 2H, ^3J = 8.8 Hz, 6′/5′-H), 8.23 (d, ^3J = 8.8 Hz, 2H, 5′/6′-H), 8.15 (d, ^3J = 7.8 Hz, 4H, 15′-H), 7.98 (d, ^3J = 8.4 Hz, 2H, 8′-H), 7.69 (brs, 2H, f′-, f′′-H), 7.56 (d, ^3J = 7.8 Hz, 2H, e′-, e′′-H), 7.47 (d, ^3J = 7.8 Hz, 2H, c′-, c′′-H), 7.36-7.42 (m, 6H, d′-, d′′-, 14′-H), 7.29 (s, 4H, 17′-H), 7.03 (s, 4H, 9′-H), 6.89 (brs, 4H, b′-H), 5.66 (brs at −60 °C, 4H, a′-H), 2.61 (s, 6H, 18′-H), 2.43 (s, 12H, g′′-, g′-H), 2.13 (s, 12H, 12′-H), 2.38 (s, 6H, 11′-H), 2.14 (s, 12H, 13′-H), 2.10 (s, 12H, 10′-H), 1.79 (s, 12H, 16′-H); **ESI-MS:** *m/z* (%) = 1244.7 (100) $[[Cu_2(\mathbf{S})(\mathbf{R})]^{2+}]$; **UV-Vis:** λ_{abs} (CH_2Cl_2) = 429, 559, 602, 607 nm; $\varepsilon_{429} = 1.96 \times 10^4$ $M^{-1}cm^{-1}$; **Elemental analysis:** ($C_{156}H_{122}Br_2Cu_2F_{12}N_{10}P_2Zn$): Calculated: C, 67.42; H, 4.43; N, 5.04. Found: C, 67.50; H, 4.41; N, 5.26.

Complex C5^1 = $[Cu(1)]^+$

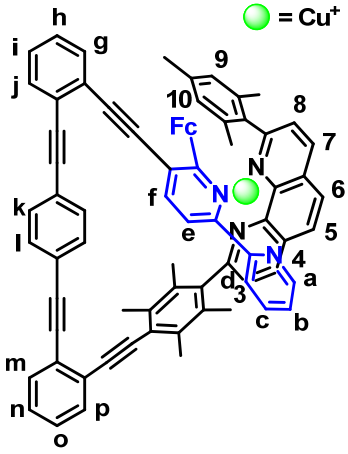

Switch **1** (0.770 mg, 0.704 µmol) and $[Cu(CH_3CN)_4]PF_6$ (0.263 mg, 0.705 µmol) were placed into an NMR tube. To this mixture, 500 µL of CD_2Cl_2 was added and subsequently the NMR was recorded. **Yield**: Quantitative; **^{1}H NMR (400 MHz, CD_2Cl_2):** δ = 8.65 (d, ^3J = 8.0 Hz, 1H, 7/4-H), 8.63 (d, ^3J = 8.0 Hz, 1H, 4/7-H), 8.19 (s, 2H, 5-, 6-H), 8.03 (dd, ^3J = 4.6 Hz, ^4J = 1.2 Hz, 1H, a-H), 7.80 (td, ^3J = 8.0 Hz, ^4J = 1.2 Hz, 1H, c-H), 7.77 (d, ^3J = 8.0 Hz, 2H, 3-, 8-H), 7.66-7.72 (m, 3H, d-, m-, p-H), 7.60-7.64 (m, 3H, g-, j-, f-H), 7.51 (s, 4H, k-, l-H), 7.46-7.48 (m, 2H, n-, o-H), 7.40-7.42 (m, 2H, h-, i-H), 7.31 (ddd, ^3J = 8.0 Hz, ^3J = 4.8 Hz, ^4J = 1.2 Hz, 1H, b-H), 7.29 (d, ^3J = 8.4 Hz, 1H, e-H), 6.43 (s, 1H, 10/9-H), 6.35 (s, 1H, 9/10-H), 4.92 (bs, 1H, Fc-H), 4.54 (bs, 1H, Fc-H), 3.89 (bs, 5H, Fc-H), 3.67 (bs, 1H, Fc-H), 3.32 (bs, 1H, Fc-H), 2.17 (s, 3H, duMe-H), 1.97 (s, 3H, mesMe-H), 1.68 (s, 3H, duMe-H), 1.78 (s, 3H, mesMe-H), 1.73 (s, 3H, duMe-H), 1.65 (s, 3H, mesMe-H), 1.53 (s, 3H, duMe-H) ppm; **ESI-MS:** *m/z* (%) = 1156.3 (100) $[Cu(\mathbf{1})]^+$.

Complex C6[1] **= [Zn(1)]**$^{2+}$

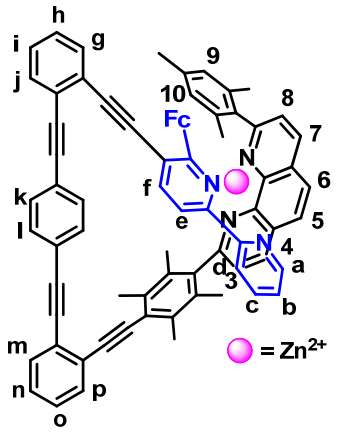

In an NMR tube, ligand **1** (0.613 mg, 0.561 µmol) was dissolved in 425 µL of CD_2Cl_2. Thereafter, $Zn(OTf)_2$ (0.204 mg, 0.562 µmol) was added as a standard solution in CD_3CN. Subsequently, ^{1}H NMR was measured without purification. **Yield**: Quantitative; **^{1}H NMR (400 MHz, CD_2Cl_2:CD_3CN (5:1)):** δ = 9.12 (d, ^3J = 8.4 Hz, 1H, 7/4-H), 8.92 (d, ^3J = 8.4 Hz, 1H, 4/7-H), 8.71 (d, ^3J = 5.2 Hz, 1H, a-H), 8.45 (d, ^3J = 8.8 Hz, 1H, 6/5-H), 8.39 (d, ^3J = 8.8 Hz, 1H, 5/6-H), 8.20 (td, ^3J = 7.8 Hz, ^4J = 1.2 Hz, 1H, c-H), 8.17 (d, ^3J = 8.4 Hz, 1H, 8/3-H), 8.02 (d, ^3J = 8.0 Hz, 1H, d-H), 7.93 (d, ^3J = 8.4 Hz, 1H, 3/8-H), 7.89 (d, ^3J = 8.4 Hz, 1H, f-H), 7.81-7.83 (m, 1H, p-H), 7.74 (ddd, ^3J = 7.8 Hz, ^3J = 5.2 Hz, ^4J = 1.2 Hz, 1H, b-H), 7.63-7.67 (m, 3H, g-, j-, m-H), 7.62 (s, 4H, k-, l-H), 7.58 (d, ^3J = 8.4 Hz, 1H, e-H), 7.54-7.56 (m, 2H, h-, i-H), 7.44-7.46 (m, 2H, n-, o-H), 6.43 (s, 1H, 10/9-H), 6.03 (s, 1H, 9/10-H), 5.48 (ddd, ^3J = 2.8 Hz, ^4J = 1.2 Hz, ^5J = 0.4 Hz, 1H, Fc-H), 4.37 (td, ^3J = 2.8 Hz, ^4J = 1.2 Hz, 1H, Fc-H), 3.98 (s, 5H, Fc-H), 3.84 (ddd, ^3J = 2.8 Hz, ^4J = 1.2 Hz, ^5J = 0.4 Hz, 1H, Fc-H), 3.35 (td, ^3J = 2.8 Hz, ^4J = 1.2 Hz, 1H, Fc-H), 2.22 (s, 3H, mesMe-H), 1.89 (s, 3H, duMe-H), 1.86 (s, 6H, duMe-H), 1.83 (s, 3H, mesMe-H), 1.71 (s, 3H, duMe-H), 1.53 (s, 3H, mesMe-H),ppm; **ESI-MS:** *m/z* (%) = 578.2 (35) [Zn(**1**)]$^{2+}$, 1307.2 (100) [Zn(**1**)+OTf$^-$]$^+$.

3. Model Study

Metal-ion dependent self-sorting was tested by mixing **2**, **3**, **4**, and $[Cu(CH_3CN)_4]PF_6$ (1.23 µmol) in a ratio of 1:2:1:1 in CD_2Cl_2. The subsequently measured ^{1}H NMR spectrum was compared with those of the individual complexes. The heteroleptic copper complex [Cu(**3**)(**4**)]$^+$ formed selectively. After addition of 1.0 equiv. of $Zn(OTf)_2$ (as a standard solution in CD_3CN), complexes [Zn(**3**)(**4**)]$^{2+}$ and [Cu(**2**)(**3**)]$^{2+}$ were afforded as judged by ^{1}H NMR. The former complex simulates formation of nanoswitch [Zn(**1**)]$^{2+}$, whereas the latter represents a HETPYP binding motif (= N_{py} → [Cu(phenAr_2)]$^+$, log K = 3.2),[5] which was used in nanorotor [Cu_2(**S**)(**R**)]$^{2+}$.

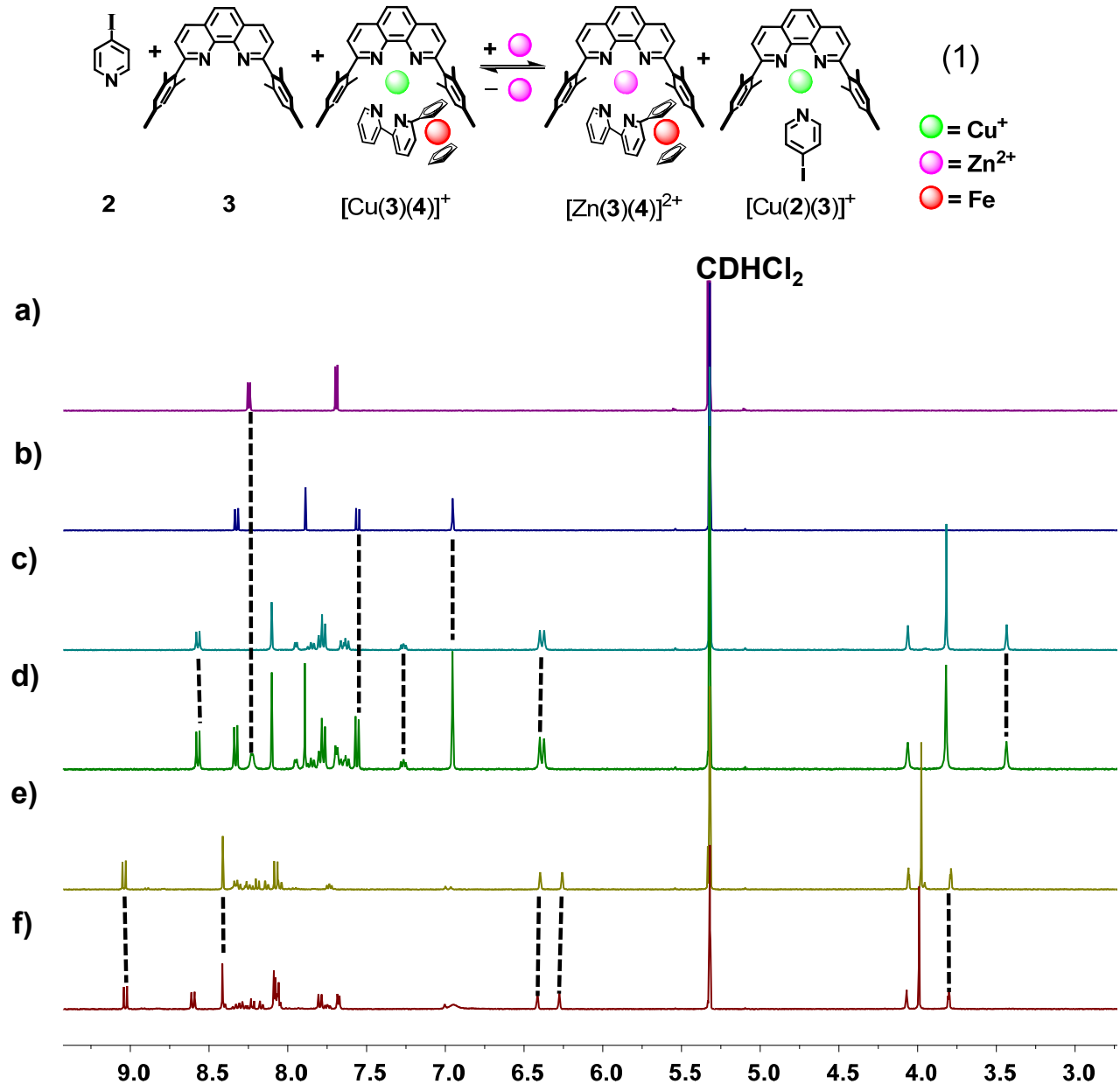

Figure S1. ^{1}H NMR (400 MHz, 298 K) of (a) **2**; (b) **3**; (c) complex [Cu(**3**)(**4**)]$^{+}$; (d) after mixing of **2**, **3**, **4** and $[Cu(CH_3CN)_4]PF_6$ in a ratio of 1:2:1:1 in CD_2Cl_2; (e) complex [Zn(**3**)(**4**)]$^{2+}$; (f) after addition of $Zn(OTf)_2$ to mixture (d).

Finally the self-sorting scenario and the translocation was tested by mixing **1**, **2**, **3** and $[Cu(CH_3CN)_4]PF_6$ (1.27 μmol) in a ratio of 1:1:1:1 in CD_2Cl_2. Subsequently, the ^{1}H NMR was measured and compared with those of the individual complexes. Accordingly, the copper complex [Cu(**1**)]$^{+}$ was afforded selectively whereas **2** and **3** remain free in the solution. After addition of 1.0 equiv. of $Zn(OTf)_2$ (as a standard solution in CD_3CN) complexes [Zn(**1**)]$^{2+}$ and [Cu(**2**)(**3**)]$^{+}$ were furnished as judged by ^{1}H NMR comparison. Thus translocation of Cu(I) was confirmed.

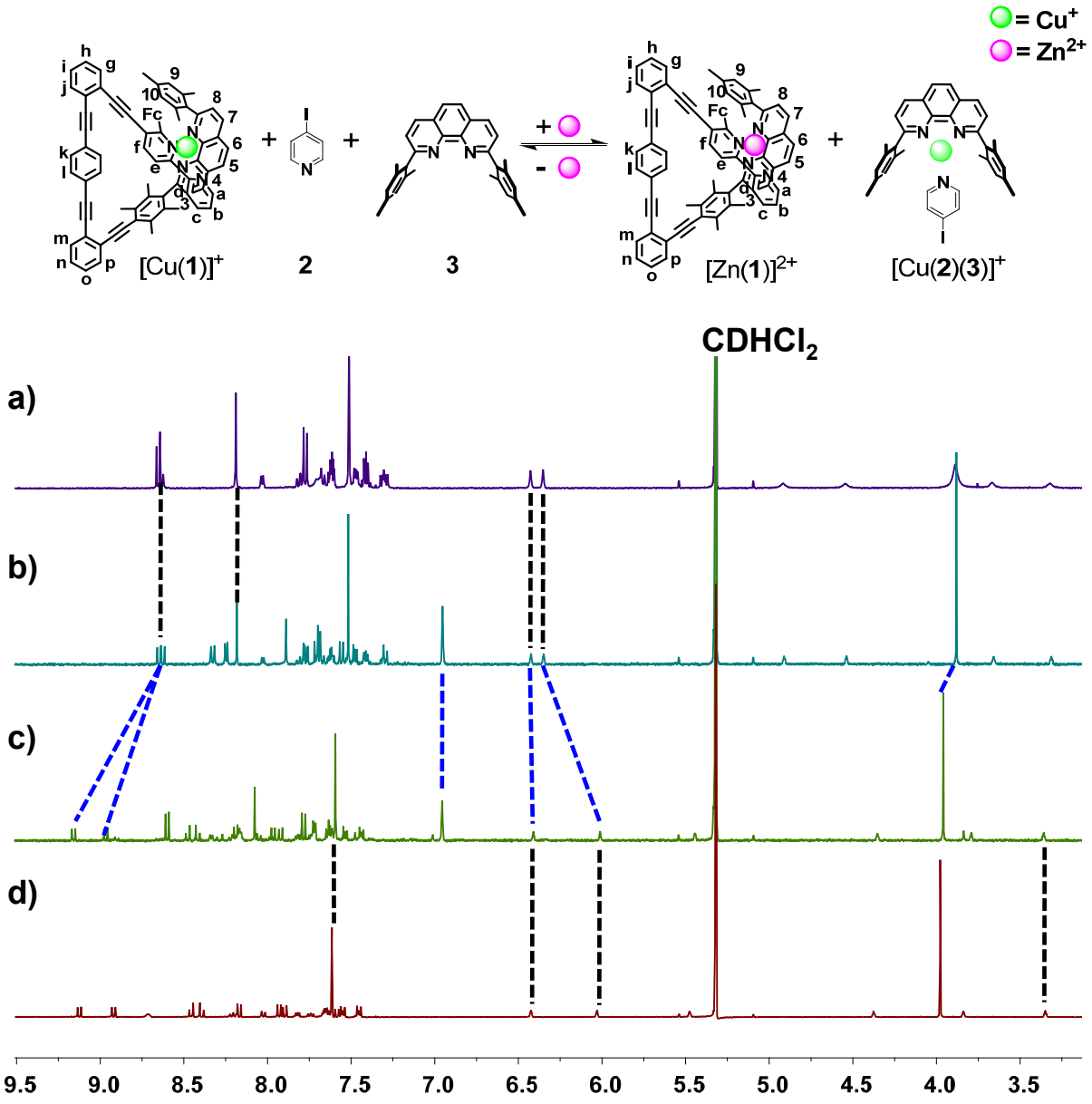

Figure S2. ^{1}H NMR (400 MHz, 298 K) of (a) complex [Cu(**1**)]$^{+}$**;** (b) after mixing of **1**, **2**, **3** and $[Cu(CH_3CN)_4]PF_6$ in a ratio of 1:1:1:1 in CD_2Cl_2; (c) after addition of $Zn(OTf)_2$ to solution (b); (d) complex [Zn(**1**)]$^{2+}$ for comparison.

4. NMR spectra: ^{1}H NMR, ^{13}C NMR, ^{1}H-^{1}H COSY

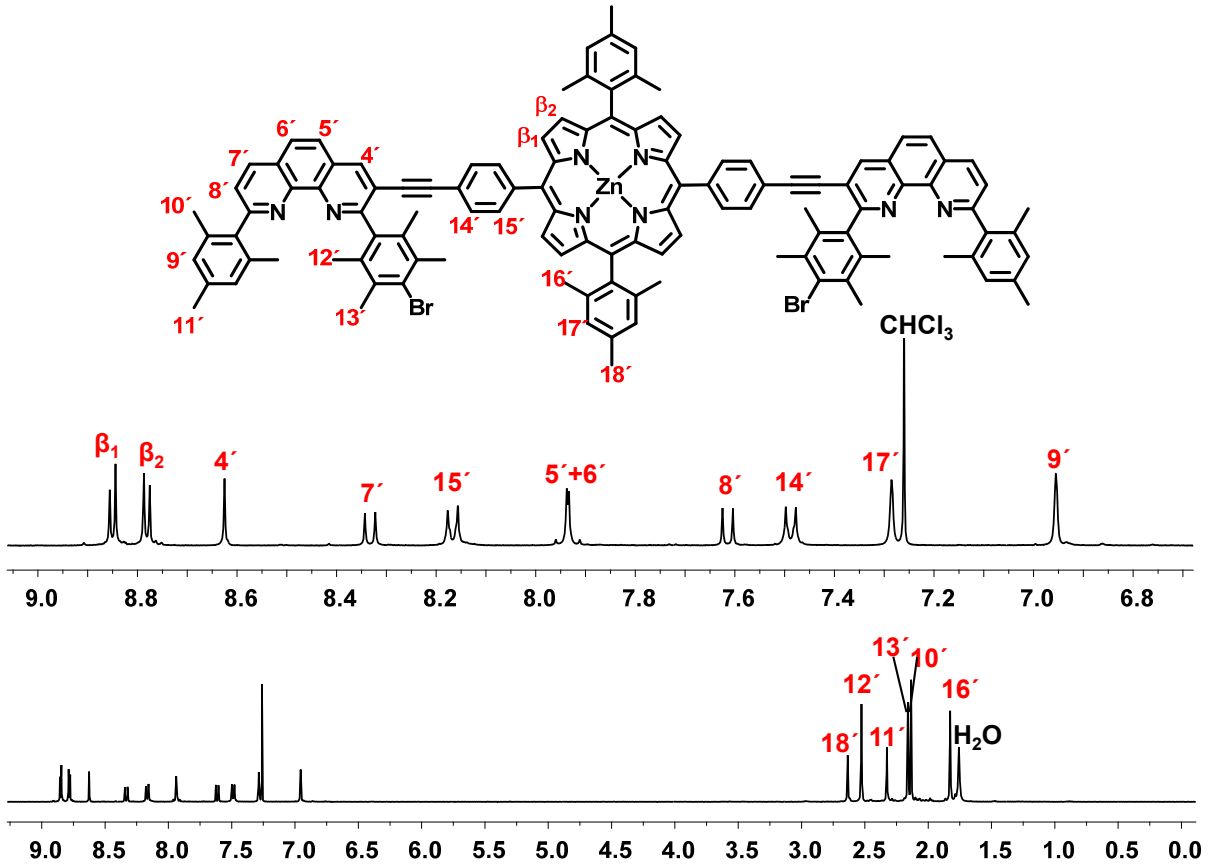

Figure S3. ^{1}H NMR spectrum of stator **S** in $CDCl_3$ (400 MHz, 298 K).

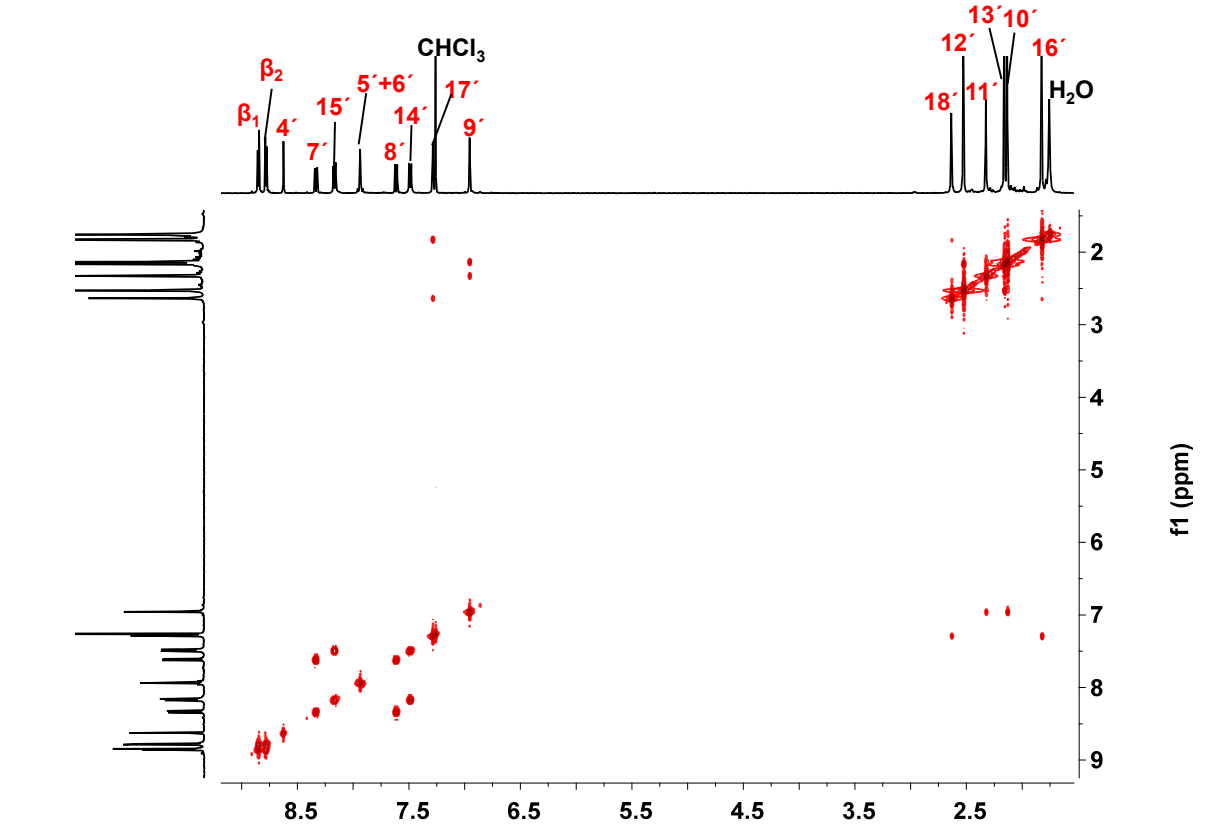

Figure S4. ^{1}H-^{1}H COSY spectrum of stator **S** in $CDCl_3$ (400 MHz, 298 K).

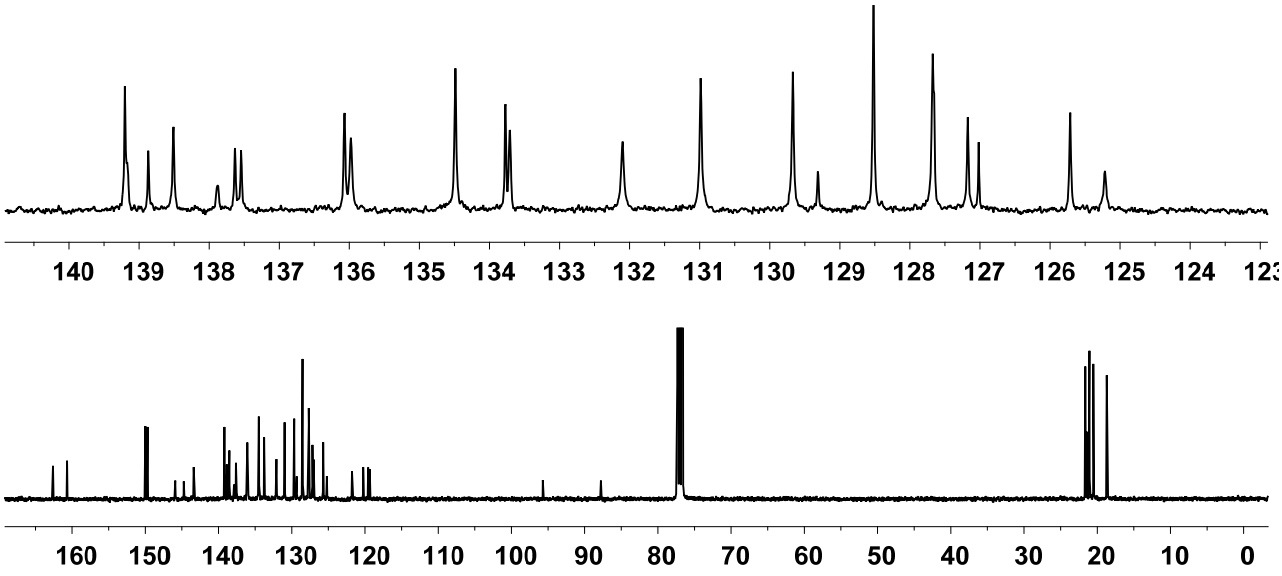

Figure S5. ^{13}C NMR spectrum of stator **S** in $CDCl_3$ (100 MHz, 298 K).

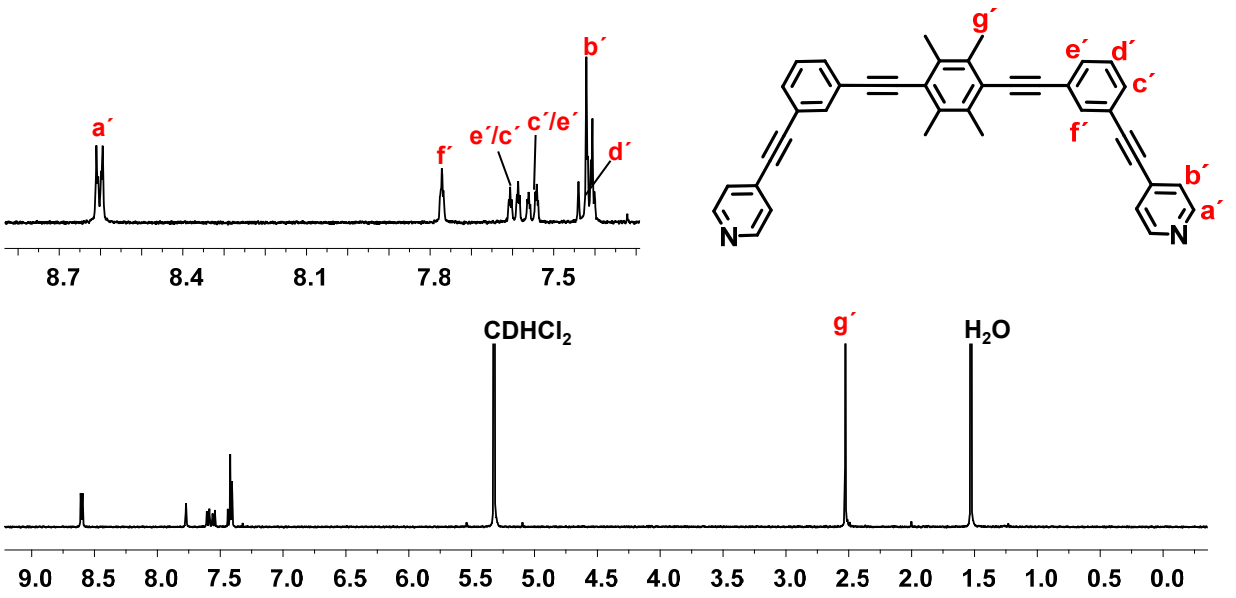

Figure S6. ^{1}H NMR spectrum of rotator ligand **R** in CD_2Cl_2 (400 MHz, 298 K).

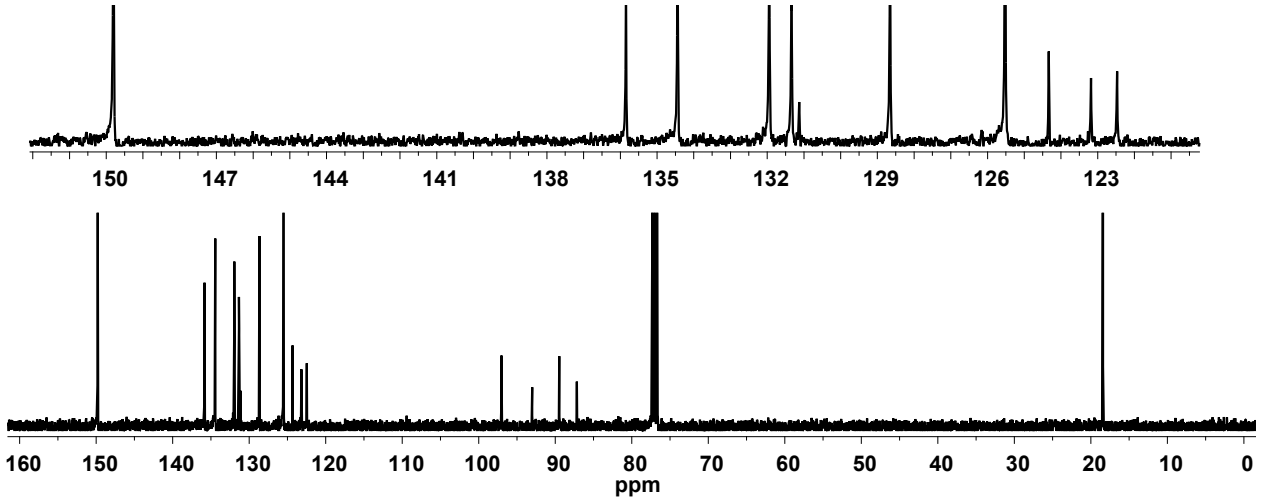

Figure S7. ^{13}C NMR spectrum of rotator **R** in $CDCl_3$ (100 MHz, 298 K).

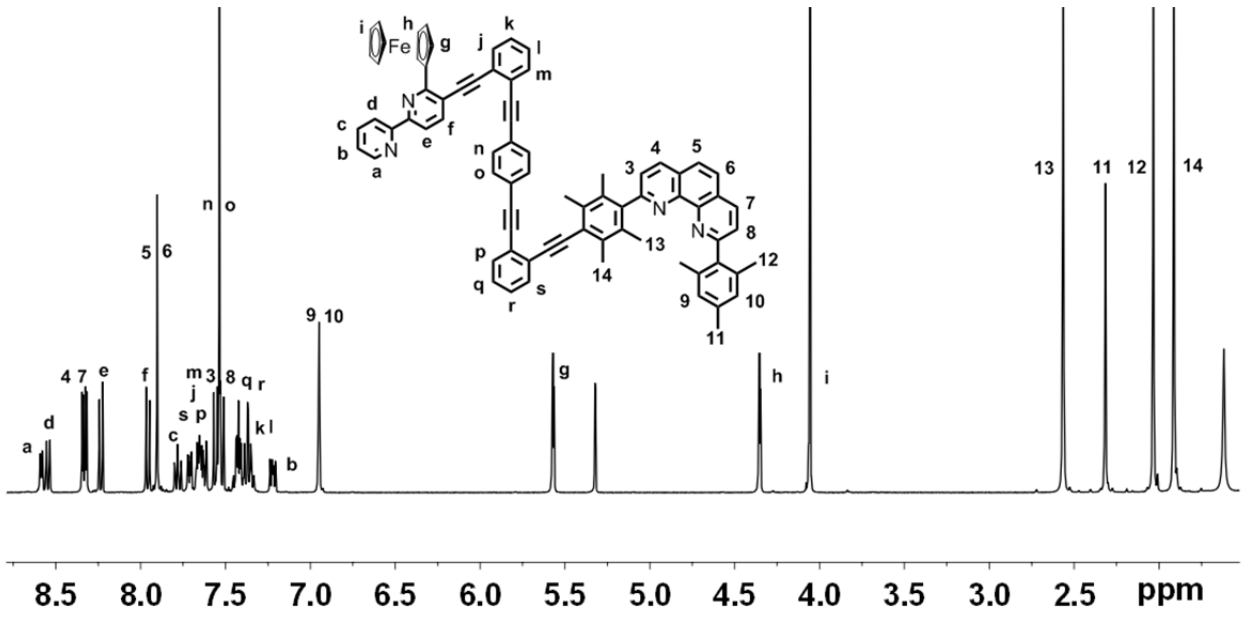

Figure S8. ^{1}H NMR spectrum of nanoswitch **1** in CD_2Cl_2 (400 MHz, 298 K).

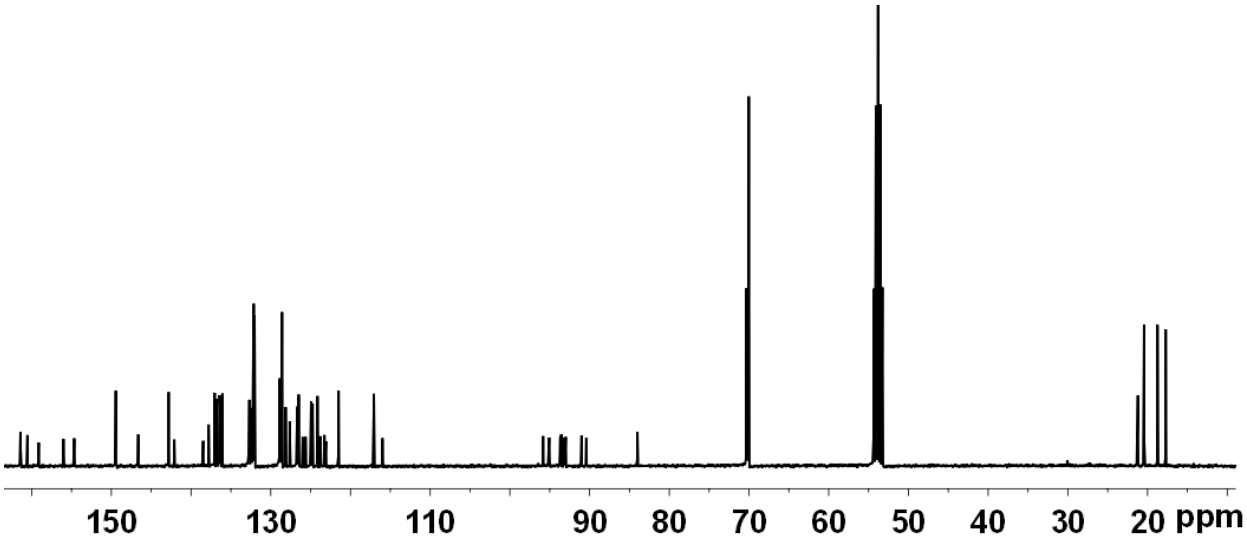

Figure S9. ^{13}C NMR spectrum of nanoswitch **1** in CD_2Cl_2 (100 MHz, 298 K).

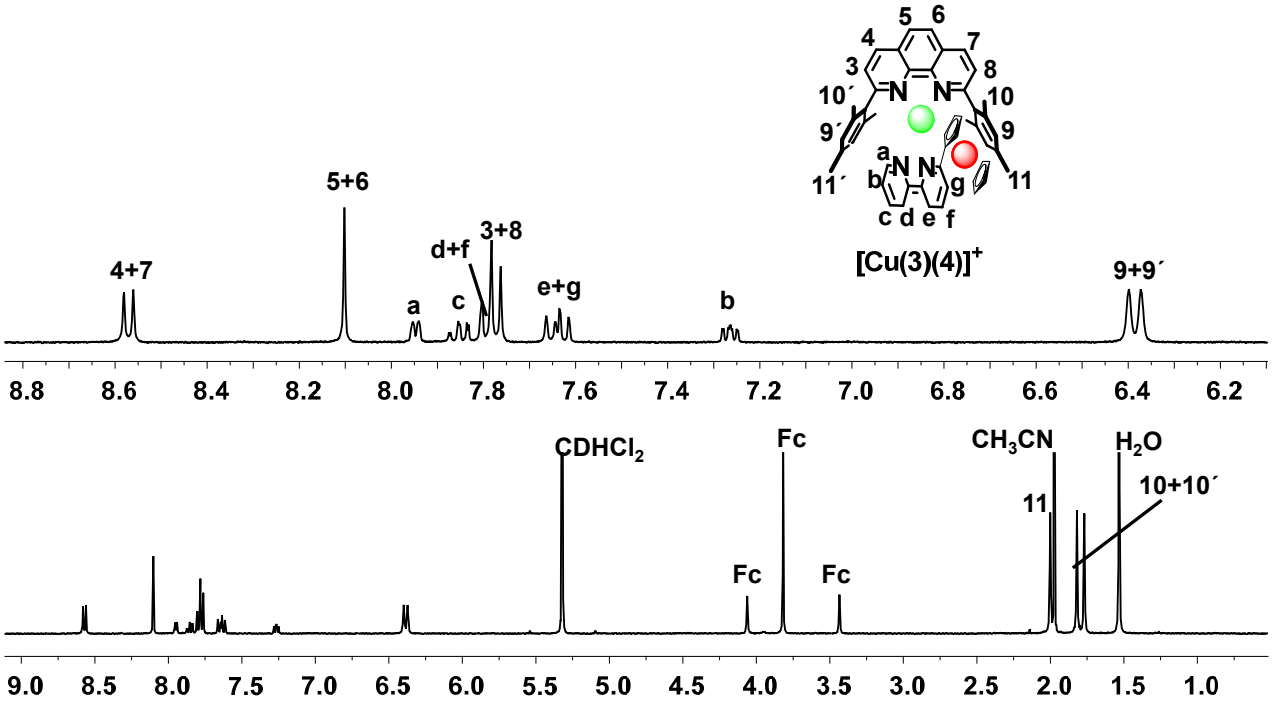

Figure S10. ^{1}H NMR spectrum of complex $[Cu(\mathbf{3})(\mathbf{4})]^{+}$ in CD_2Cl_2 (400 MHz, 298 K).

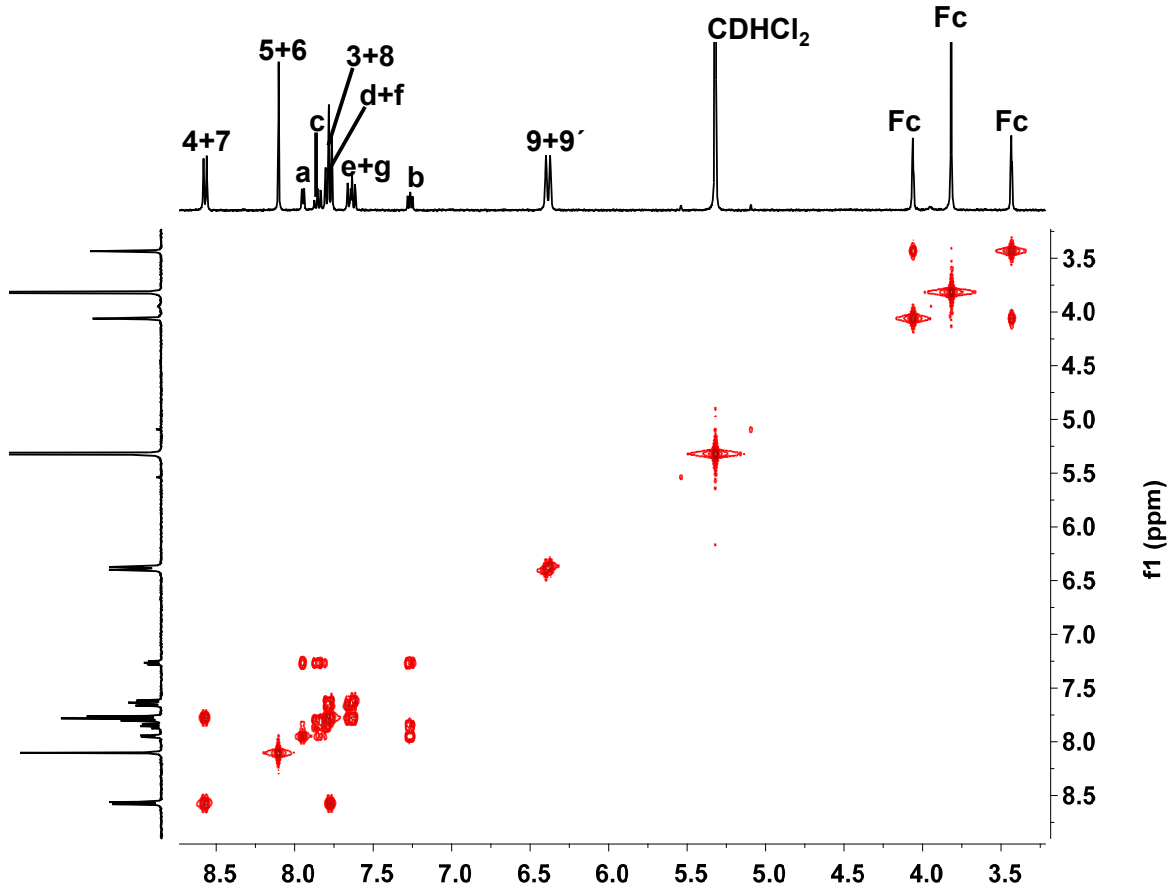

Figure S11. ^{1}H-^{1}H COSY spectrum of $[Cu(\mathbf{3})(\mathbf{4})]^{+}$ in CD_2Cl_2 (400 MHz, 298 K).

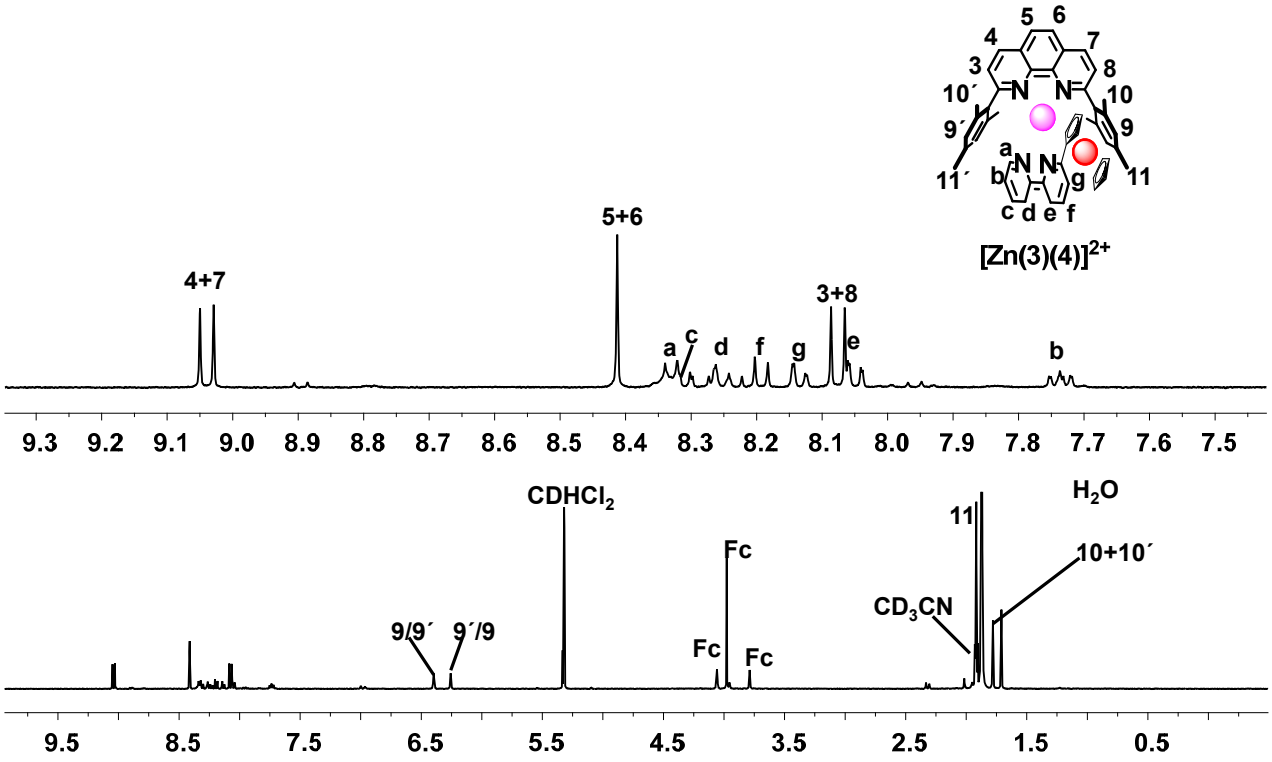

Figure S12. ^{1}H NMR spectrum (400 MHz, 298 K) of complex $[Zn(\mathbf{3})(\mathbf{4})]^{2+}$ in CD_2Cl_2:CD_3CN (9:1).

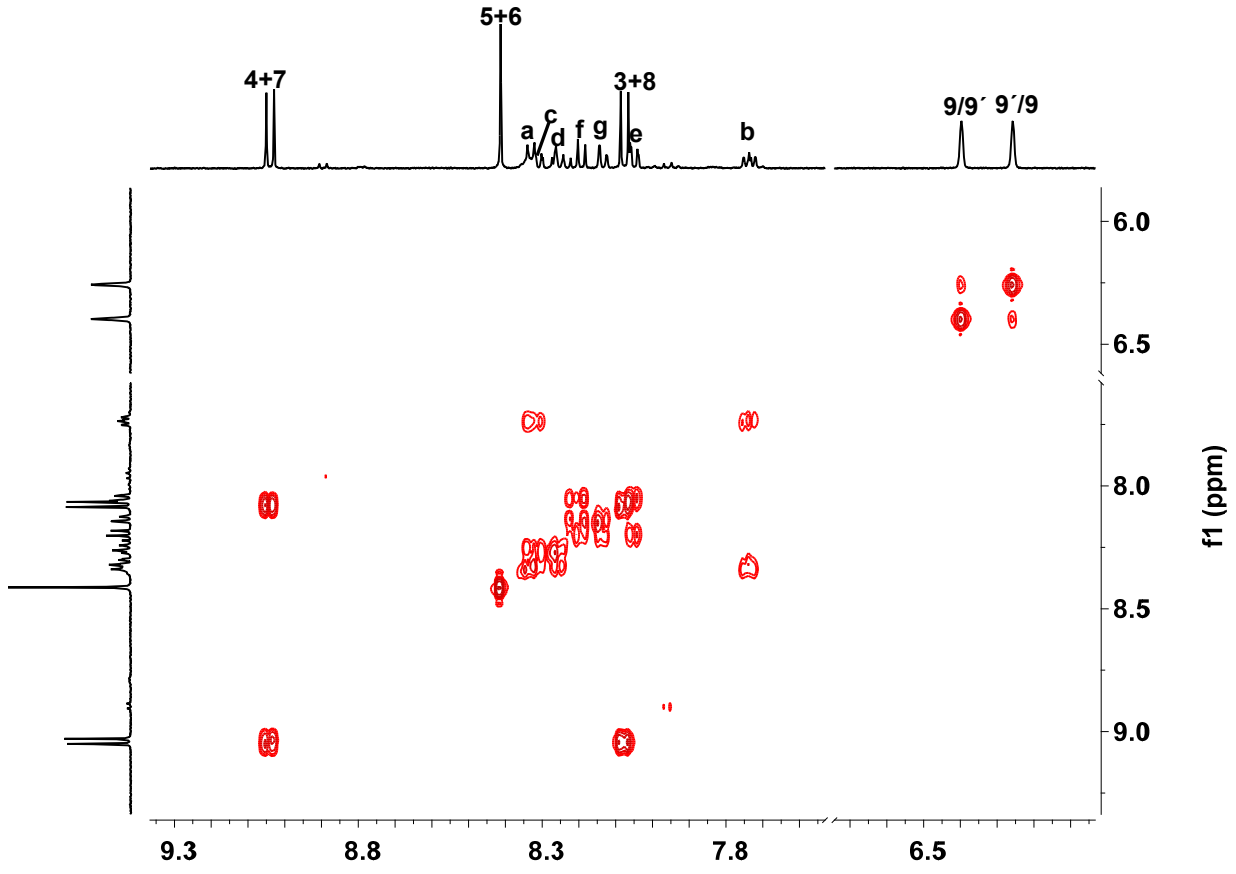

Figure S13. ^{1}H-^{1}H COSY spectrum (400 MHz, 298 K) of [Zn(**3**)(**4**)]$^{2+}$ in CD_2Cl_2:CD_3CN (9:1).

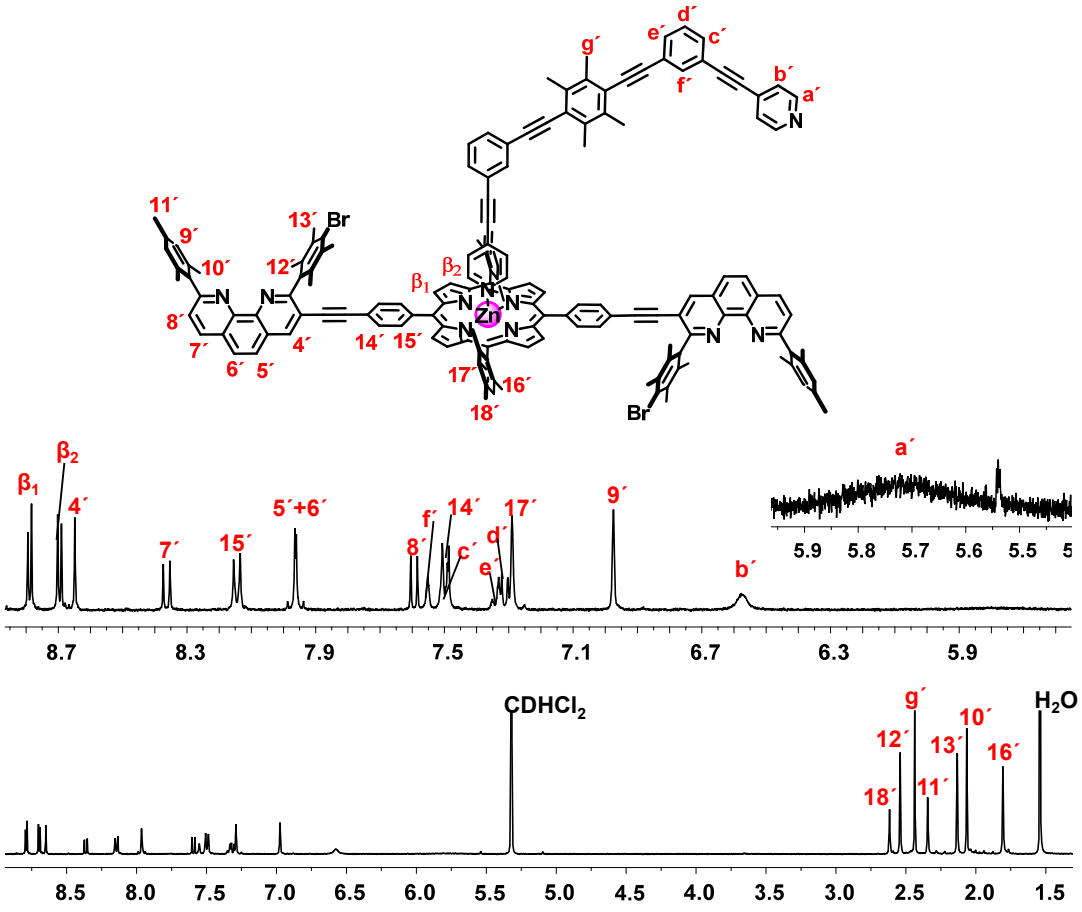

Figure S14. ^{1}H NMR spectrum (400 MHz, 298 K) of complex [(**S**)•(**R**)] in CD_2Cl_2.

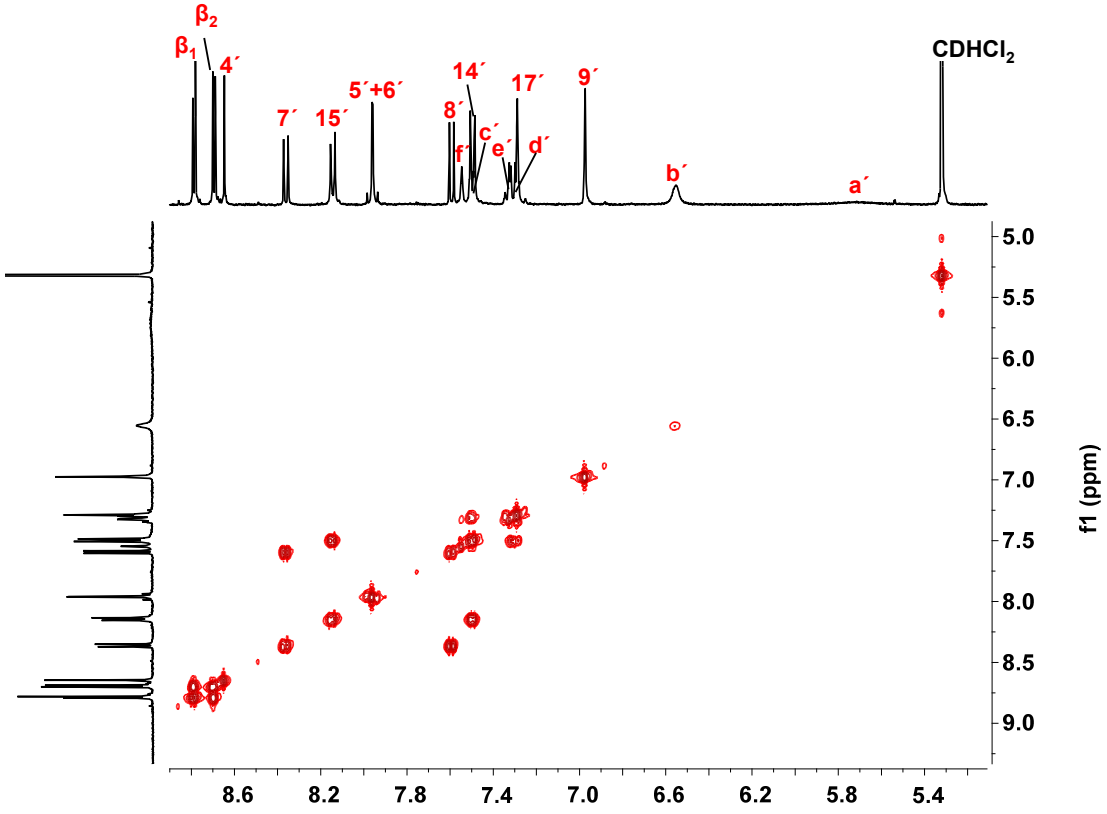

Figure S15. ^{1}H-^{1}H COSY spectrum (400 MHz, 298 K) of complex [(**S**)•(**R**)] in CD_2Cl_2.

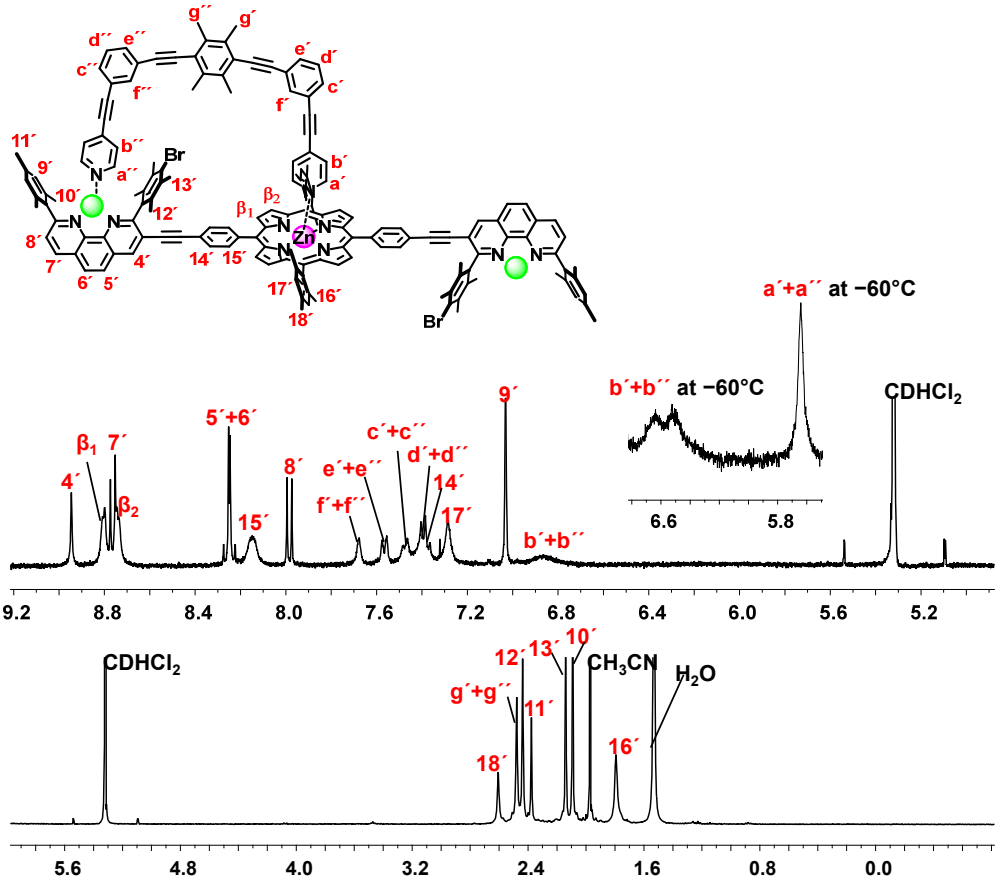

Figure S16. ^{1}H NMR spectrum (400 MHz, 298 K) of complex $[Cu_2(\mathbf{S})(\mathbf{R})]^{2+}$ in CD_2Cl_2.

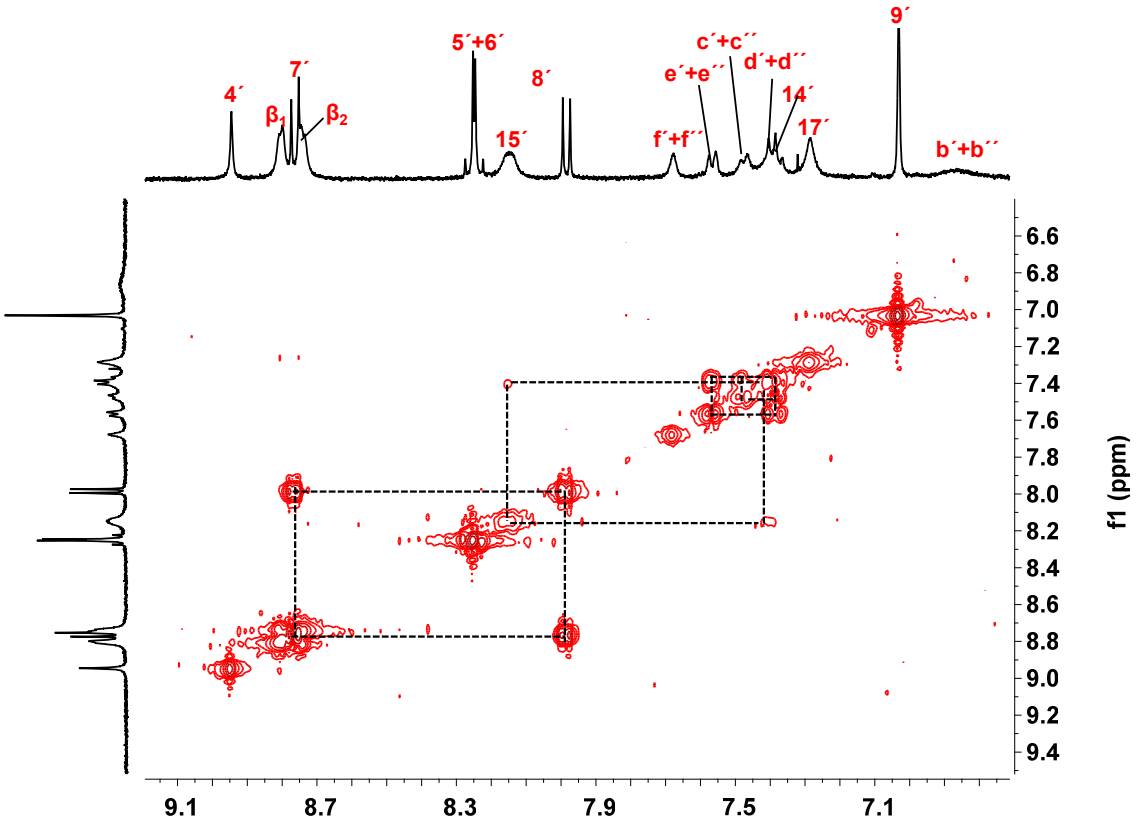

Figure S17. ^{1}H-^{1}H COSY spectrum (400 MHz, 298 K) of complex $[Cu_2(\mathbf{S})(\mathbf{R})]^{2+}$ in CD_2Cl_2.

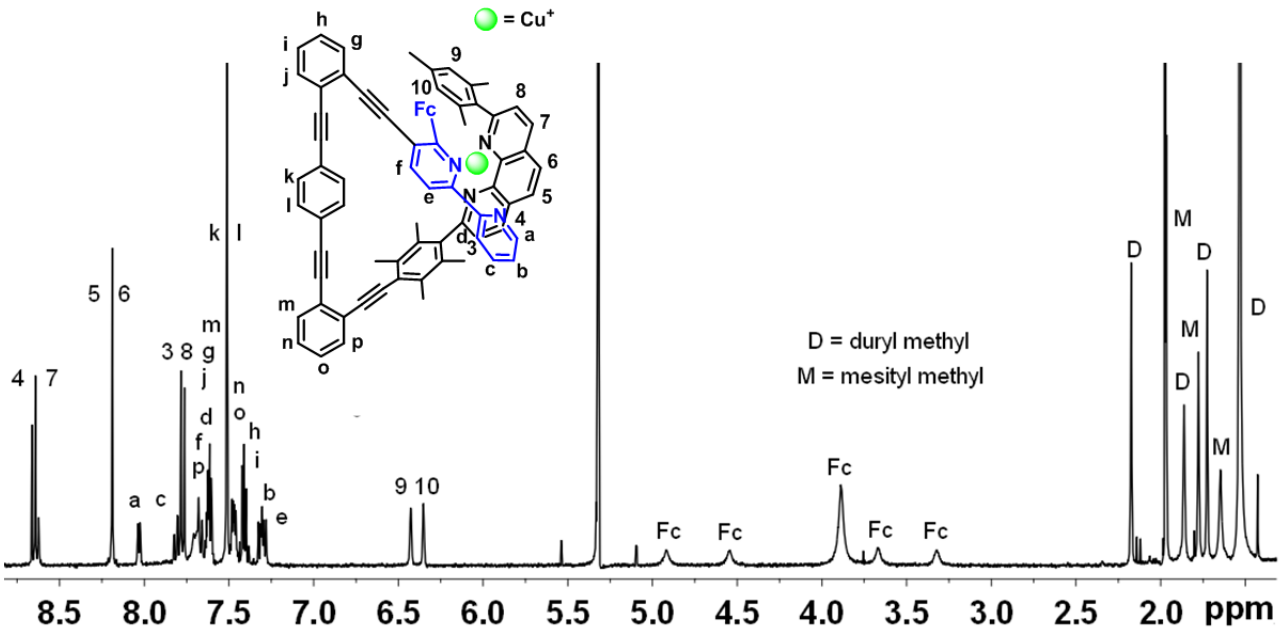

Figure S18. ^{1}H NMR spectrum (400 MHz, 298 K) of complex $[Cu(\mathbf{1})]^{+}$ in CD_2Cl_2.

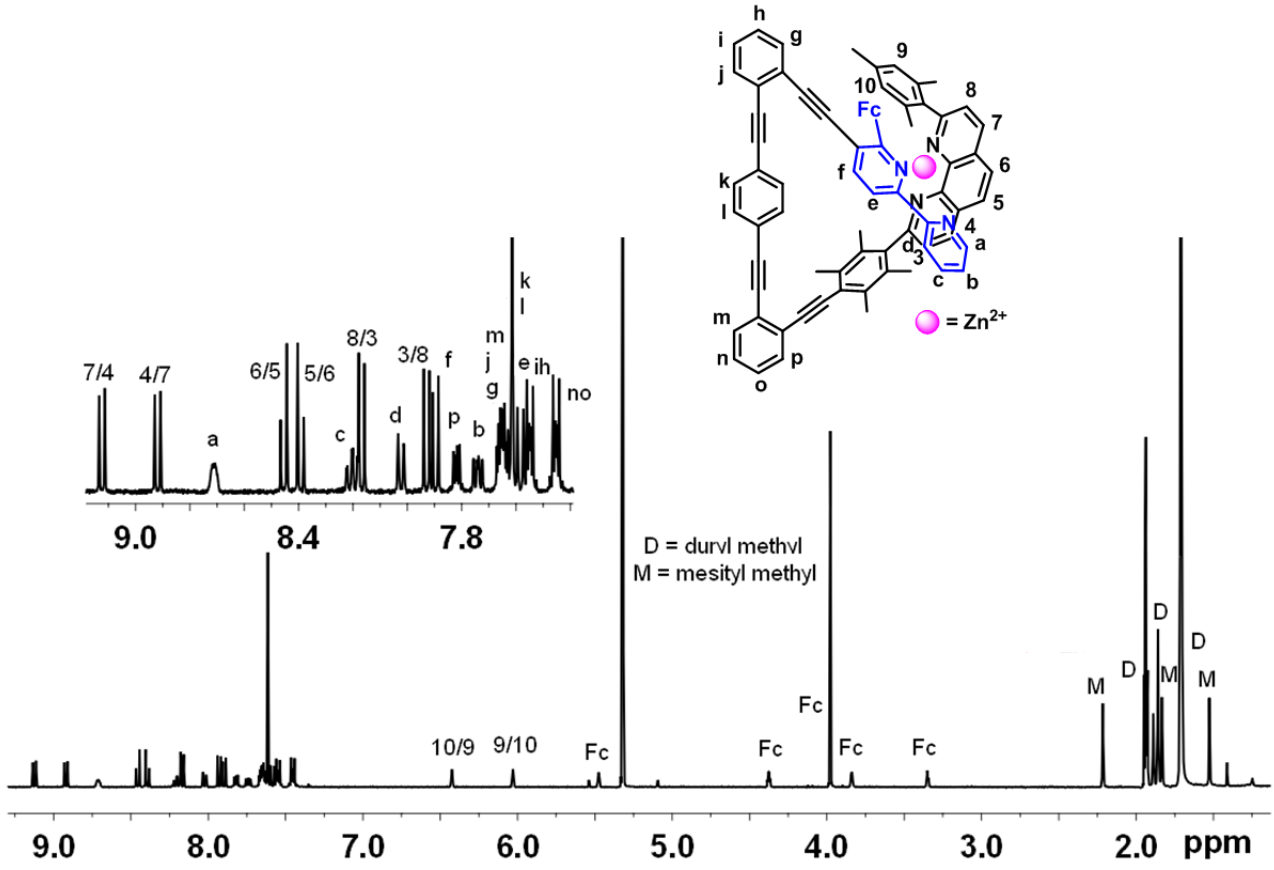

Figure S19. ^{1}H NMR spectrum (400 MHz, 298 K) of complex $[Zn(\mathbf{1})]^{2+}$ in CD_2Cl_2:CD_3CN (5:1).

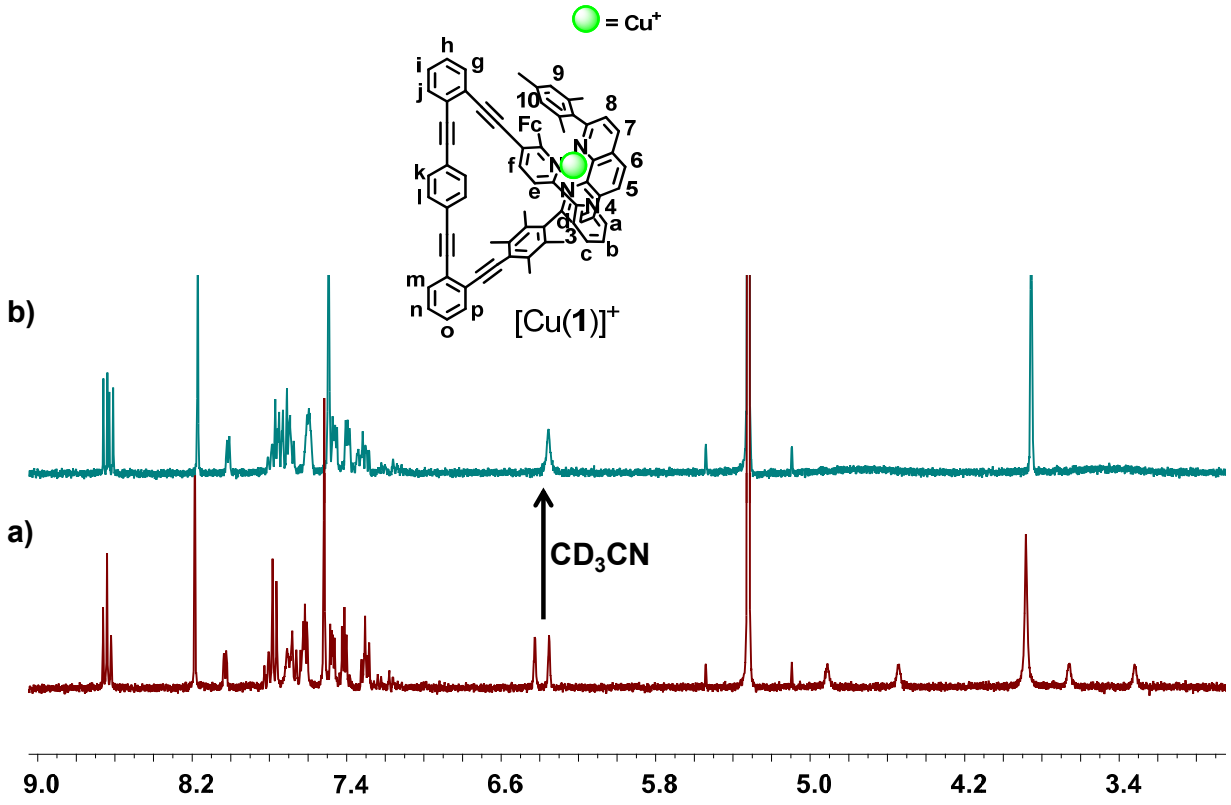

Figure S20. ^{1}H NMR spectrum (400 MHz, 298 K) of (a) complex $[Cu(\mathbf{1})]^{+}$ in CD_2Cl_2, (b) after addition of 60 µL of CD_3CN to the same complex. Now mesityl protons 9-H and 10-H show up as a broad singlet at 6.36 ppm.

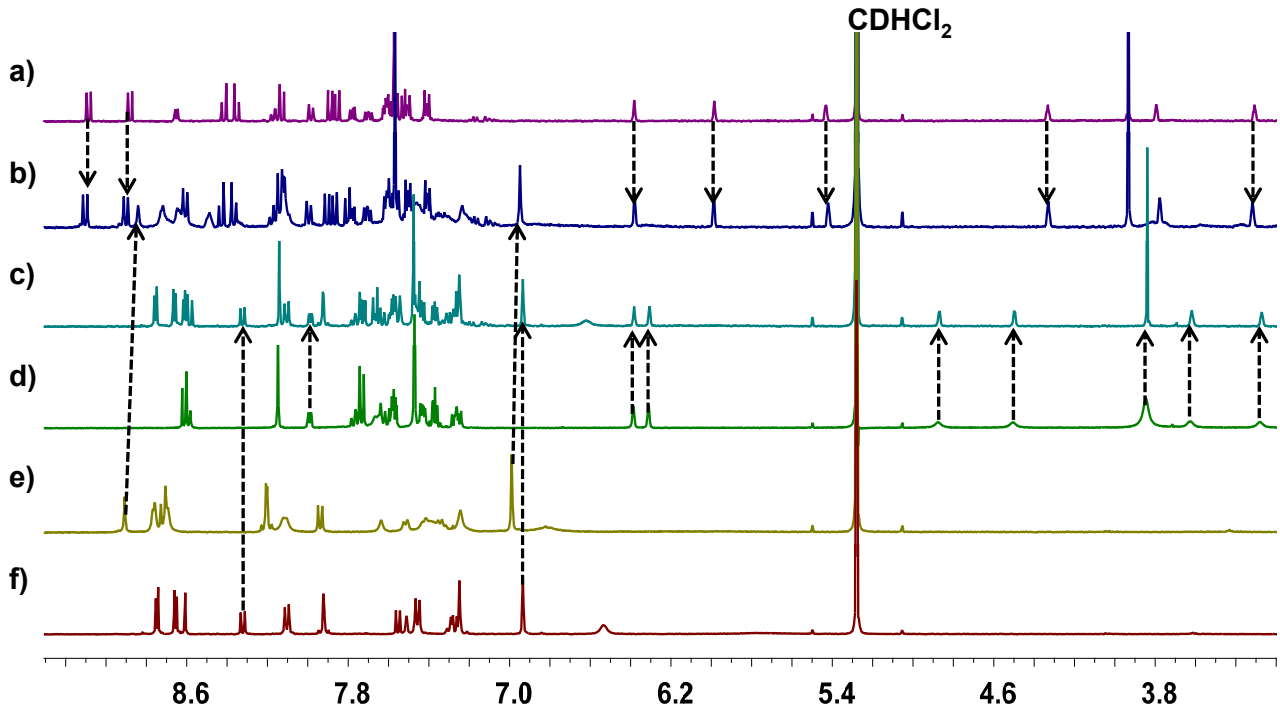

Figure S21. Partial ^{1}H NMR (400 MHz, in CD_2Cl_2) of (a) $[Zn(\mathbf{1})]^{2+}$; (b) **NetState II**: mixture of $[Cu_2(\mathbf{S})(\mathbf{R})]^{2+}$ and $[Zn(\mathbf{1})]^{2+}$; (c) **NetState I**: mixture of $[Cu(\mathbf{1})]^{+}$ and $[(\mathbf{S})\bullet(\mathbf{R})]$. (d) $[Cu(\mathbf{1})]^{+}$; (e) $[Cu_2(\mathbf{S})(\mathbf{R})]^{2+}$; (f) $[(\mathbf{S})\bullet(\mathbf{R})]$.

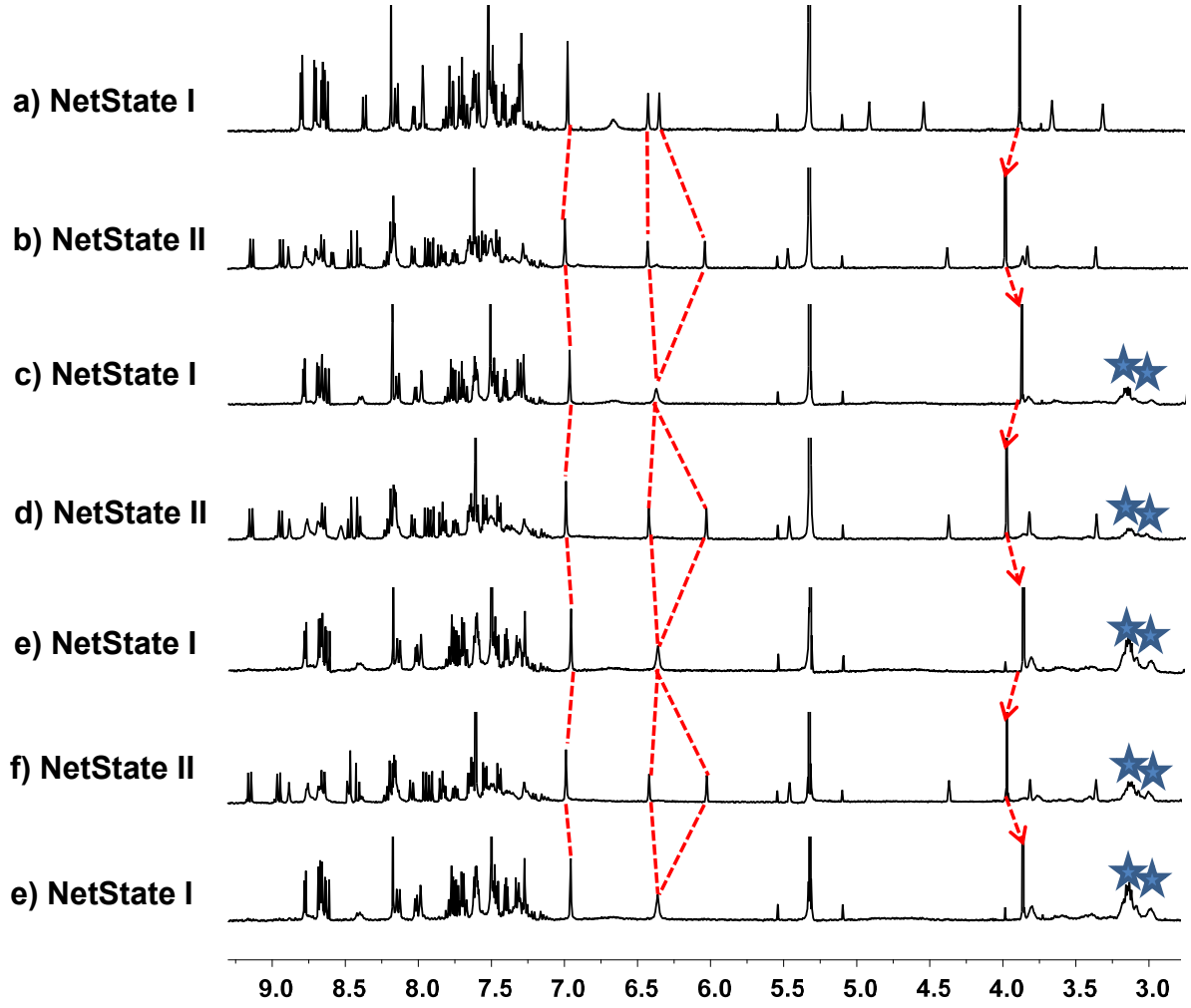

Figure S22. ^{1}H NMR spectra (400 MHz, CD_2Cl_2, 298 K) showing the reversible switching between **NetState I** and **II** over 2 cycles. The different NMR traces represent: (a) after mixing of switch **1**, **S**, **R** and $[Cu(CH_3CN)_4]PF_6$ (1.8×10^{-3} M) in 2:1:1:2 ratio (**NetState I**); (b) after adding 2.0 equiv. of $Zn(OTf)_2$ as a standard solution in CD_3CN, furnishing $[Zn(\mathbf{1})]^{2+}$ and $[Cu_2(\mathbf{S})(\mathbf{R})]^{2+}$ (**NetState II**); (c) NMR after addition of 2.0 equiv. of hexacyclen to produce **NetState I**; (d) after adding another 2.0 equiv. of $Zn(OTf)_2$ (**NetState II**); (e) NMR after addition of 2.0 equiv. of hexacyclen; (f) after adding another 2.0 equiv. of $Zn(OTf)_2$ (**NetState II**); (g) NMR after addition of 2.0 equiv. of hexacyclen. Blue asterisk marked signals are from $[Zn(hexacyclen)]^{2+}$ complex.

Mechanism of metal translocation

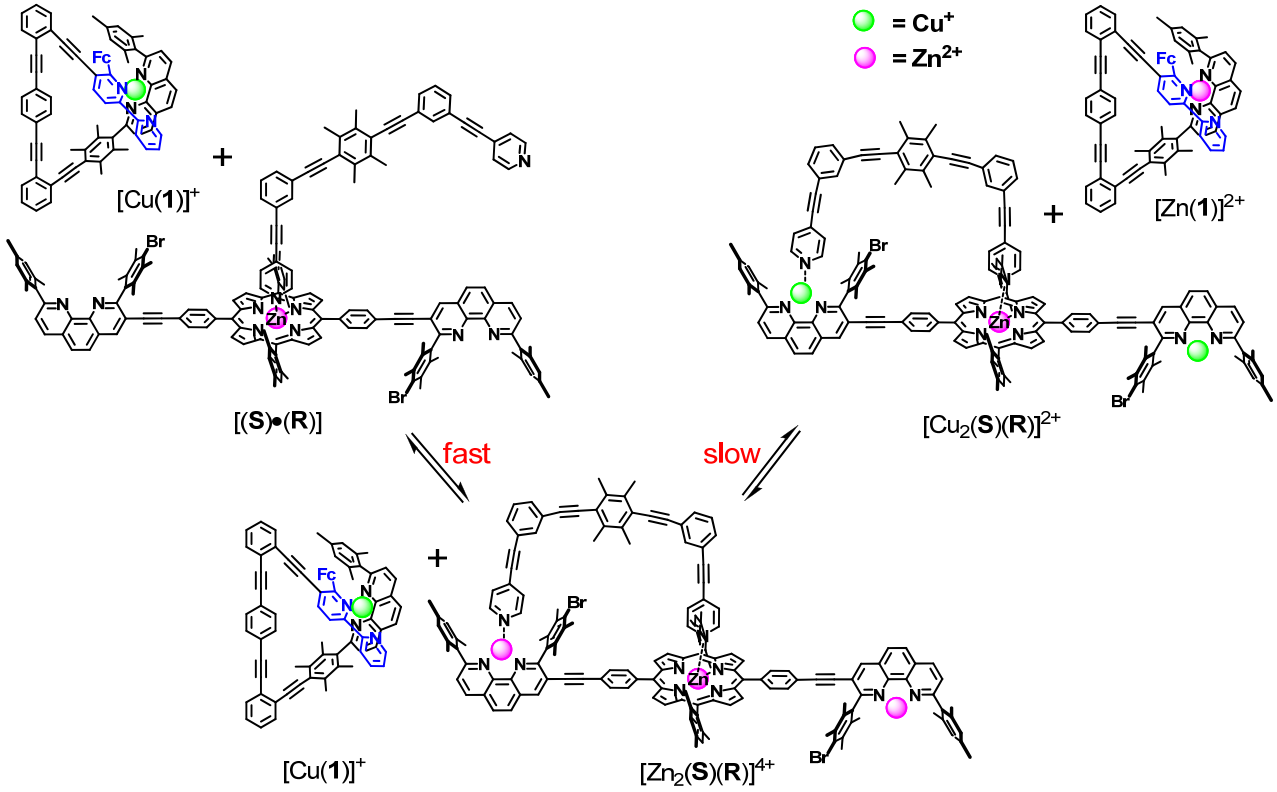

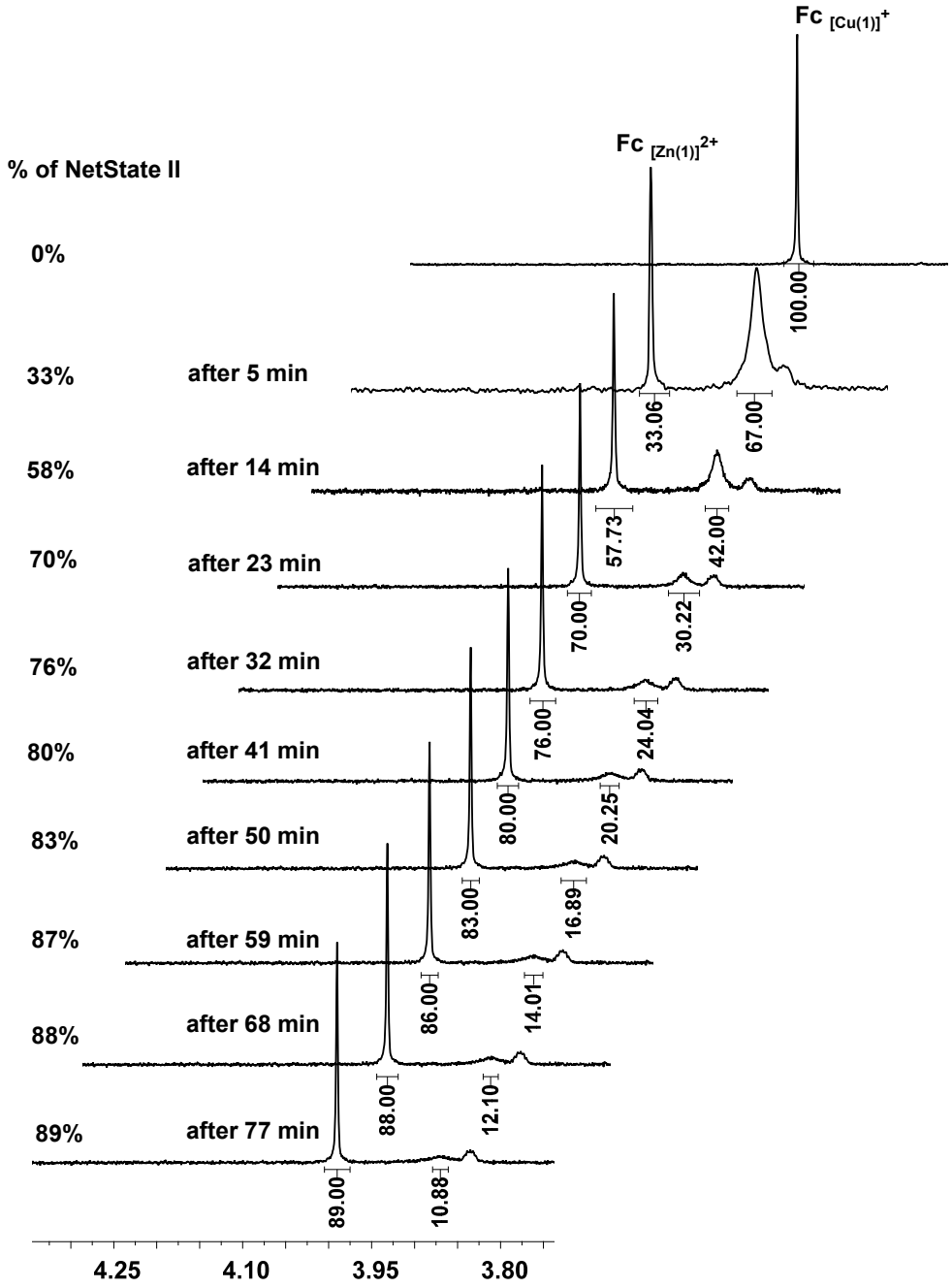

Figure S23. ^{1}H NMR spectrum (400 MHz, CD_2Cl_2:CD_3CN = 5:1) of the Cu^+ translocation at 298 K (8.9×10^{-4} M). To a solution of **NetState I** in CD_2Cl_2 in an NMR tube was added $Zn(OTf)_2$ as a standard solution in CD_3CN. Subsequently, ^{1}H NMR spectra were recorded to elucidate the metal exchange at nanoswitch **1** with time.

5. Catalytic experiments

Solid reactants were transferred to the NMR tube and dissolved in CD_2Cl_2:CD_3CN = 5:1. The mixture was heated at 50 °C for 2 h and the yield of the click (singlet at δ 5.98 ppm) was determined using 1,3,5-trimethoxybenzene (**5**) as an internal standard (singlet at δ 6.04 ppm).

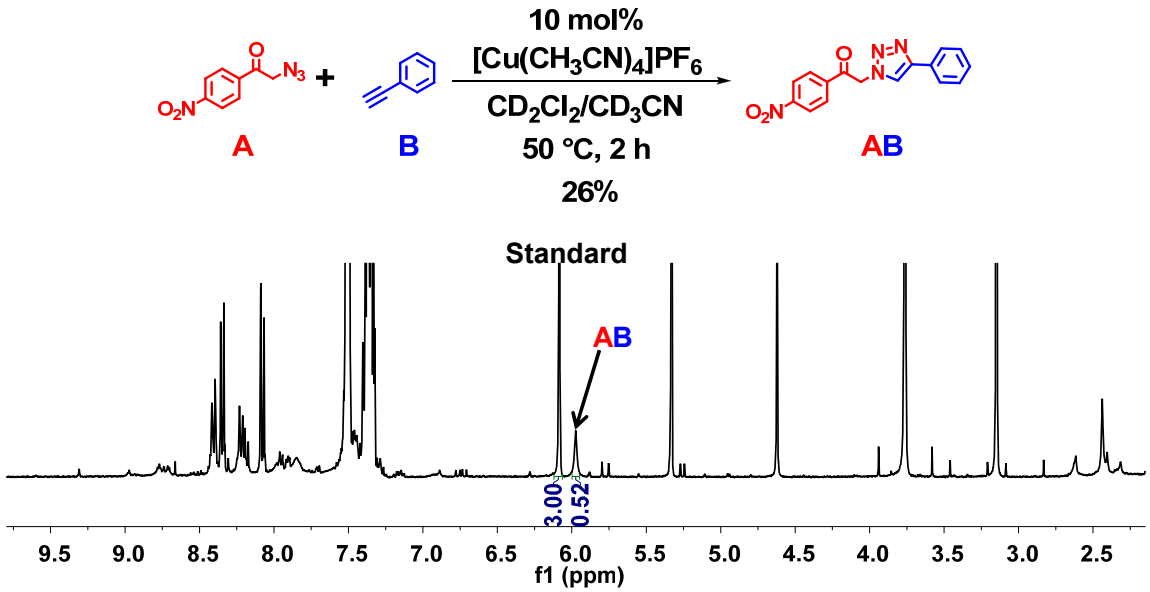

Figure S24. ^{1}H NMR (400 MHz, CD_2Cl_2:CD_3CN = 5:1, 298 K) spectrum obtained after heating the reaction mixture of (≈ 1.92 mM) $[Cu(CH_3CN)_4]PF_6$, **A**, **B** and trimethoxybenzene **5** in 1:10:50:10 ratio at 50 °C for 2 h. The integration demonstrated that **AB** was formed in 26% yield

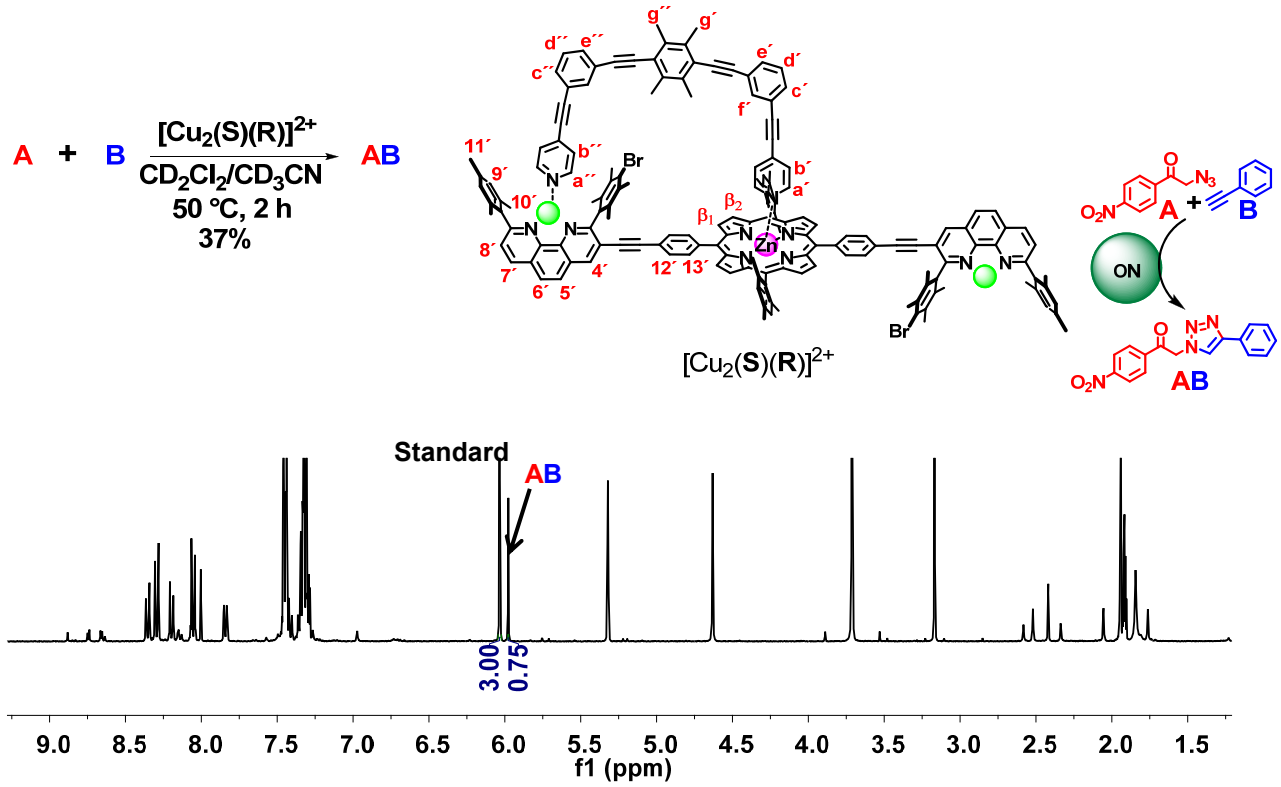

Figure S25. ^{1}H NMR (400 MHz, CD_2Cl_2:CD_3CN = 5:1, 298 K) spectrum obtained after heating the reaction mixture of stator **S** (≈ 0.96 mM), rotator **R**, $[Cu(CH_3CN)_4]PF_6$, **A**, **B** and trimethoxybenzene **5** in 1:1:2:20:100:20 ratio at 50 °C for 2 h. The integration demonstrated that **AB** was formed in 37% yield.

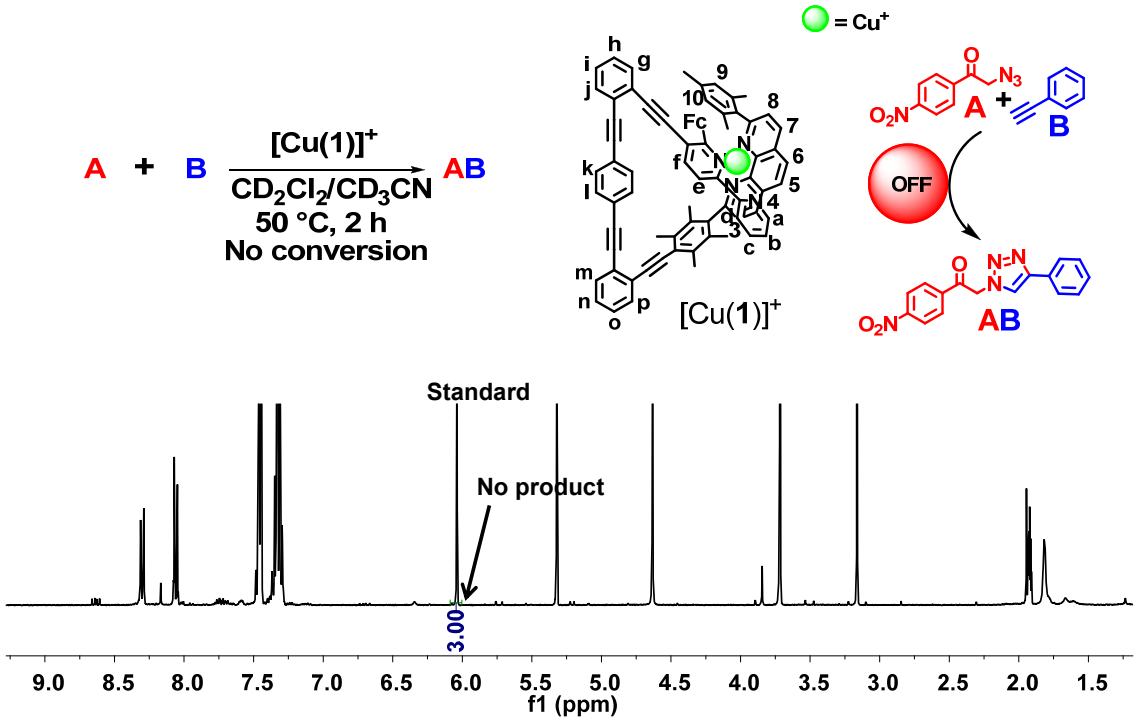

Figure S26. ^{1}H NMR (400 MHz, CD_2Cl_2:CD_3CN = 5:1, 298 K) spectrum obtained after heating the reaction mixture of nanoswitch **1** (≈ 1.92 mM), $[Cu(CH_3CN)_4]PF_6$, **A**, **B** and trimethoxybenzene **5** in 1:1: 10:100:10 ratio at 50 °C for 2 h does not show any product **AB**.

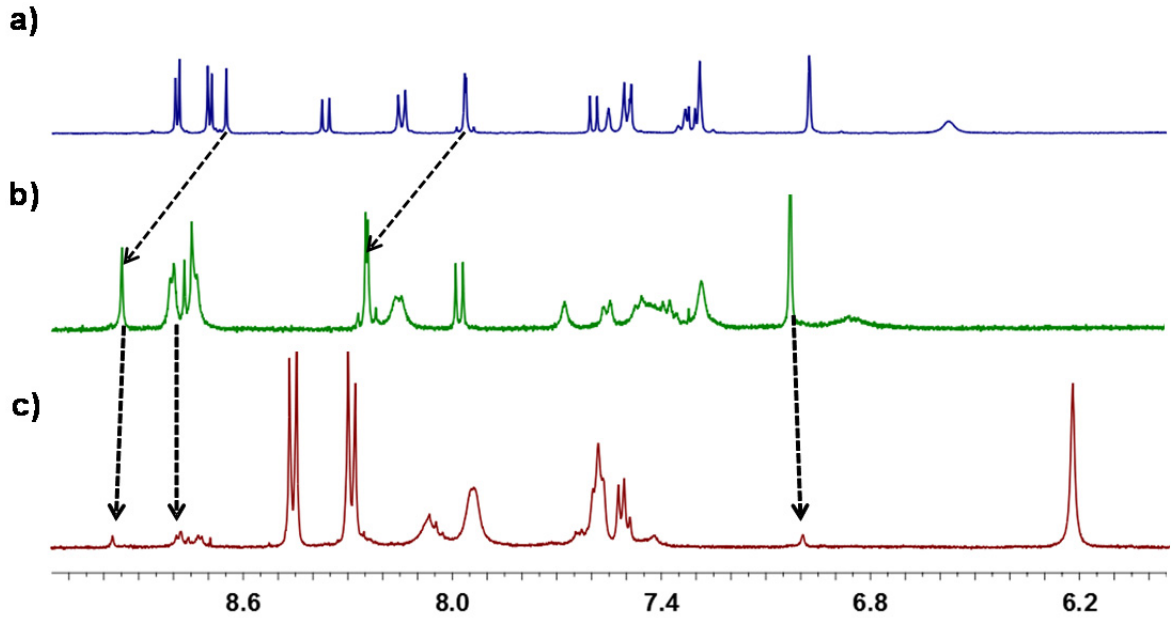

Figure S27. Partial ^{1}H-NMR (400 MHz, CD_2Cl_2, 298 K) of (a) [(**S**)•(**R**)], (b) nanorotor $[Cu_2(\mathbf{S})(\mathbf{R})]^{2+}$, (c) mixture of nanorotor $[Cu_2(\mathbf{S})(\mathbf{R})]^{2+}$ and click product **AB** in 1: 10 ratio.

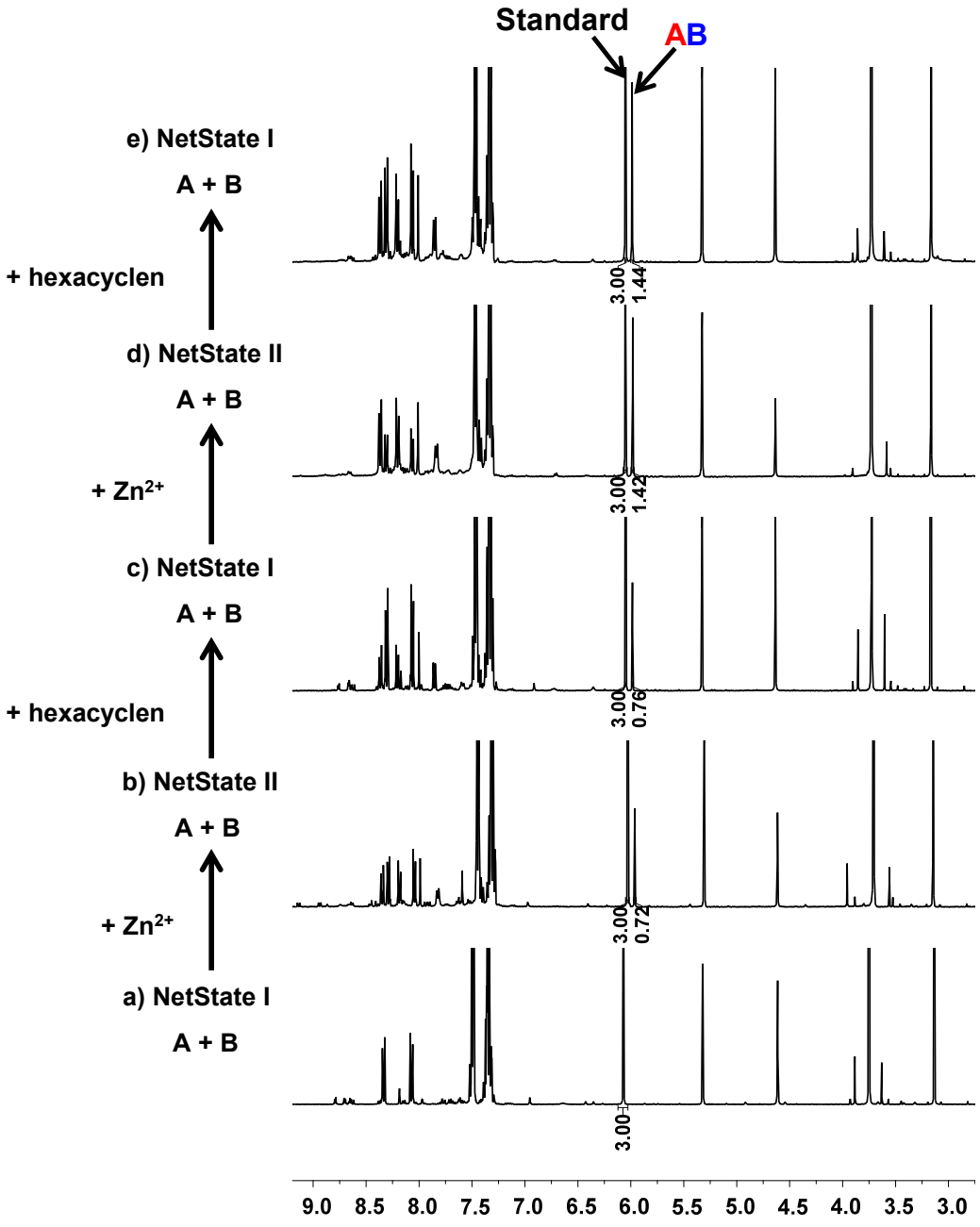

Figure S28a. Run 1 with two catalytic cycles. ^{1}H NMR (400 MHz, CD_2Cl_2:CD_3CN = 5:1, 298 K) spectrum obtained after (a) heating the reaction mixture of **1** (≈ 1.92 mM), **S**, **R**, $[Cu(CH_3CN)_4]PF_6$, **A**, **B**, **5** in a 2:1:1:2:20:100:20 ratio at 50 °C for 2 h in an NMR tube revealed that click catalysis (no singlet at δ 5.98) was OFF. (b) After addition of 2.0 equiv. of $Zn(OTf)_2$ with respect to **S** and subsequent heating at 50 °C for 2 h click product **AB** was formed (yield = 36% calculated with respect to internal standard **5**). (c) After adding 2.0 equiv. of hexacyclen with respect to **S** and heating at 50 °C for 2 h, only 2% increase in the amount of click product **AB** was observed (yield = 38%). (d) After addition of 2.0 equiv. of $Zn(OTf)_2$ with respect to **S** and heating at 50 °C for 2 h resulted in an increase of the click product **AB** by 33% (total yield = 71%). (e) After adding 2.0 equivalent of hexacyclen with respect to **S** and heating at 50 °C for 2 h, only 1% increase in the amount of click product **AB** was observed (total yield = 72%).

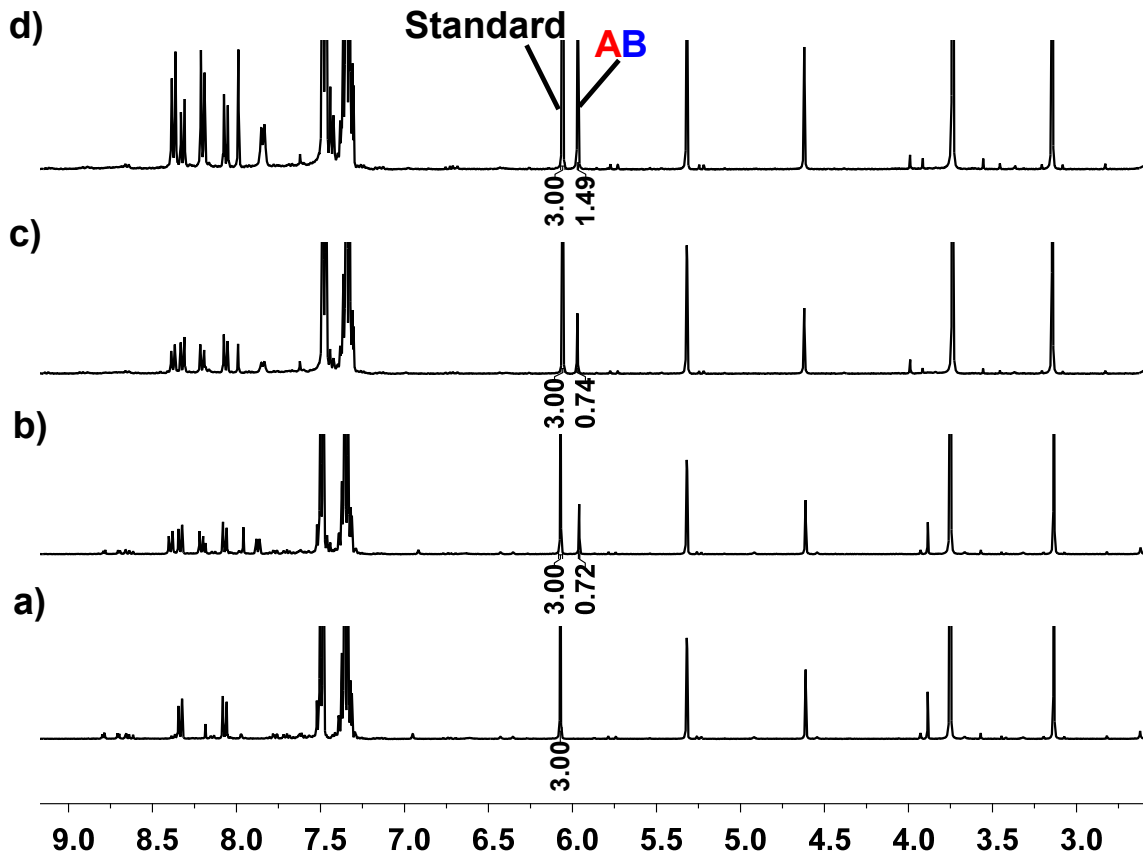

Figure S28b. Run 2 with two catalytic cycles. ^{1}H NMR (400 MHz, CD_2Cl_2:CD_3CN = 5:1, 298 K) spectrum obtained after (a) heating the reaction mixture of 1 (≈ 1.92 mM), **S**, **R**, $[Cu(CH_3CN)_4]PF_6$, **A**, **B**, **5** in a 2:1:1:2:20:100:20 ratio at 50 °C for 2 h in an NMR tube revealed that click catalysis (no singlet at δ 5.98) was OFF. (b) After addition of 2.0 equiv. of $Zn(OTf)_2$ with respect to **S** and subsequent heating at 50 °C for 2 h click product **AB** was formed (yield = 36% calculated with respect to internal standard **5**). (c) After adding 2.0 equiv. of hexacyclen with respect to **S** and heating at 50 °C for 2 h, only1% increase in the amount of click product **AB** was observed (yield = 37%). (d) After addition of 2.0 equiv. of $Zn(OTf)_2$ with respect to **S** and heating at 50 °C for 2 h resulted in an increase of the click product **AB** by 38% (total yield = 75%).

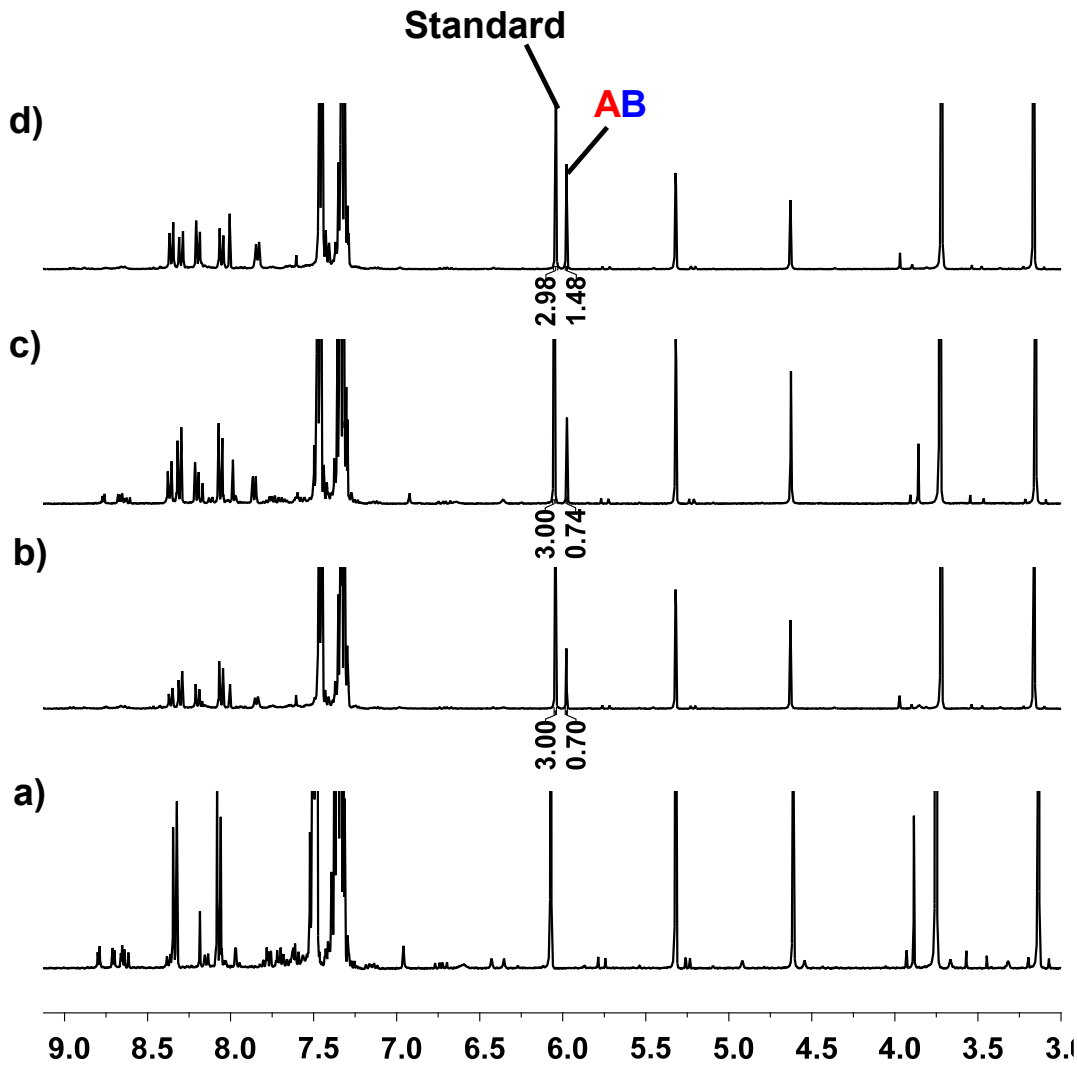

Figure S28c. Run 3 with two catalytic cycles.. ^{1}H NMR (400 MHz, CD_2Cl_2:CD_3CN = 5:1, 298 K) spectrum obtained after (a) heating the reaction mixture of **1** (≈ 1.92 mM), **S**, **R**, $[Cu(CH_3CN)_4]PF_6$, **A**, **B**, **5** in a 2:1:1:2:20:100:20 ratio at 50 °C for 2 h in an NMR tube revealed that click catalysis (no singlet at δ 5.98) was OFF. (b) After addition of 2.0 equiv. of $Zn(OTf)_2$ with respect to **S** and subsequent heating at 50 °C for 2 h click product **AB** was formed (yield = 35% calculated with respect to internal standard **5**). (c) After adding 2.0 equiv. of hexacyclen with respect to **S** and heating at 50 °C for 2 h, only 2% increase in the amount of click product **AB** was observed (yield = 37%). (d) After addition of 2.0 equiv. of $Zn(OTf)_2$ with respect to **S** and heating at 50 °C for 2 h resulted in an increase of the click product **AB** by 37% (total yield = 74%).

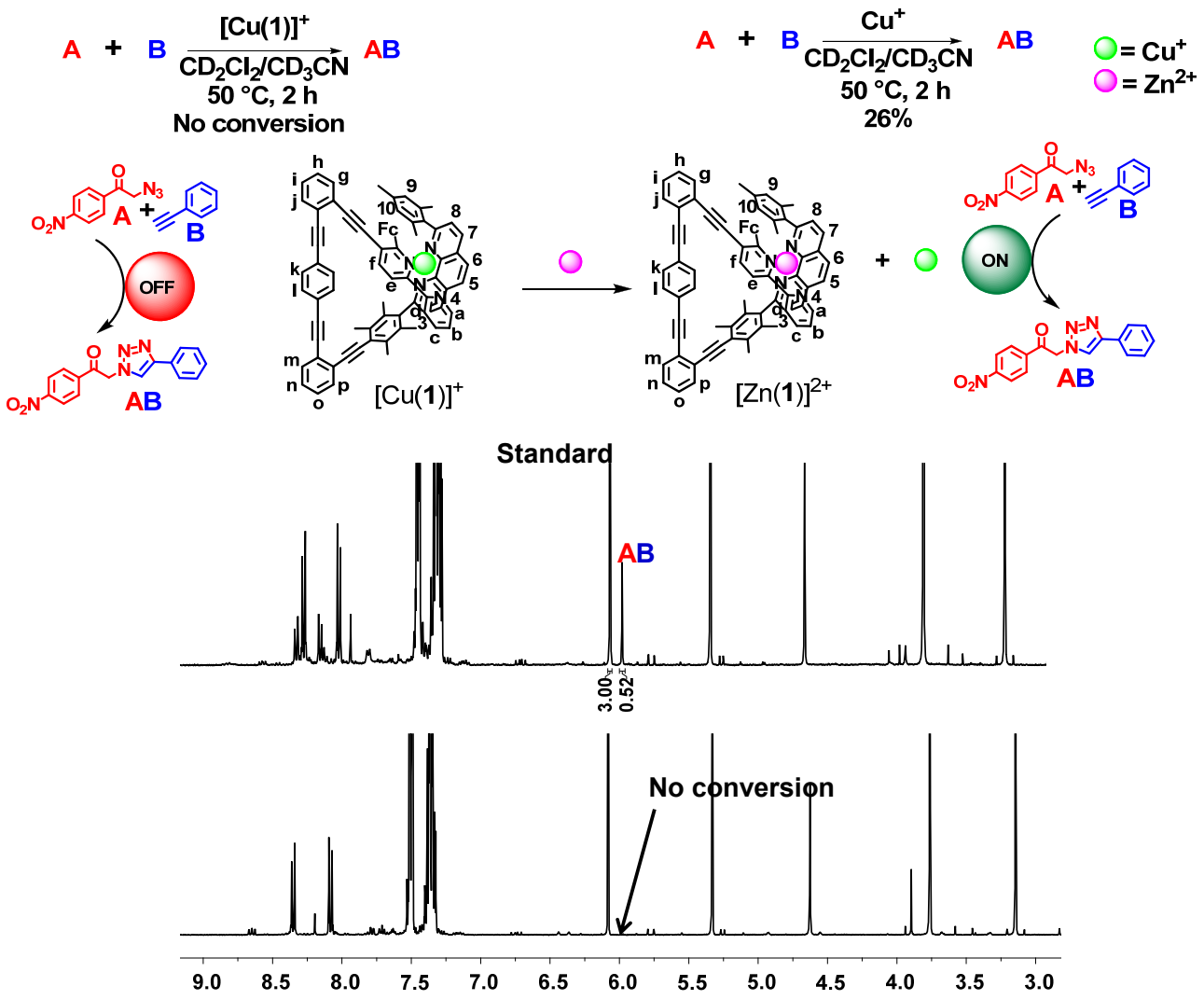

Figure S29. ^{1}H NMR (400 MHz, CD_2Cl_2:CD_3CN = 5:1, 298 K) spectrum obtained (a) after heating the reaction mixture of nanoswitch **1** (≈ 1.92 mM), $[Cu(CH_3CN)_4]PF_6$, **A**, **B** and trimethoxybenzene **5** in 1:1: 10:100:10 ratio at 50 °C for 2 h does not show any product **AB**. (b) After addition of 1.0 equiv. of $Zn(OTf)_2$ as a standard solution in CD_3CN followed by heating at 50 °C for 2 h, the yield of **AB** is 26%.

6. DOSY NMR spectra

Calculation of hydrodynamic radius from:

a) **DOSY**: The diffusion coefficient *D* for **[Zn(S)(R)]**$^{2+}$ and **[Cu(S)(R)]**$^{+}$ was obtained from their DOSY spectrum. The corresponding hydrodynamic radius was calculated by using the Stokes-Einstein equation

$$r = k_B T/6\pi\eta D$$

b) **Optimized structure**: Radius of **[**Zn**(S)(R)**$]^{2+}$ was calculated from their optimized structures at PM6 level. First a circle around the structure was considered and its radius approximated as hydrodynamic radius of the rotor. It is denoted as r_{com}.

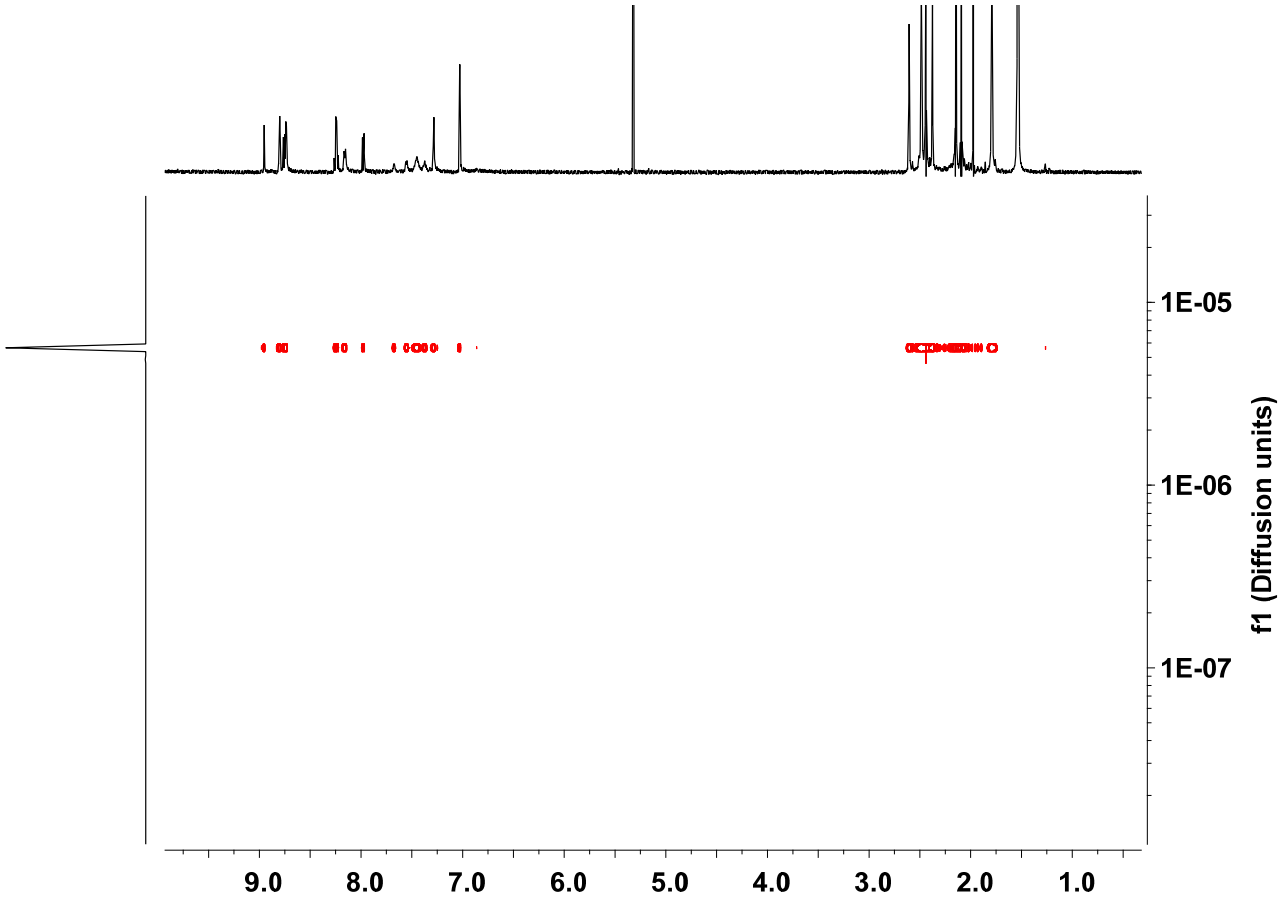

Figure S30. ^{1}H-DOSY NMR of $[Cu_2(\mathbf{S})(\mathbf{R})]^{2+}$ in CD_2Cl_2 (600 MHz, 298K). Diffusion coefficient $D = 3.6 \times 10^{-10}$ m^2 s^{-1}, Hydrodynamic radius r ~14.7 Å.

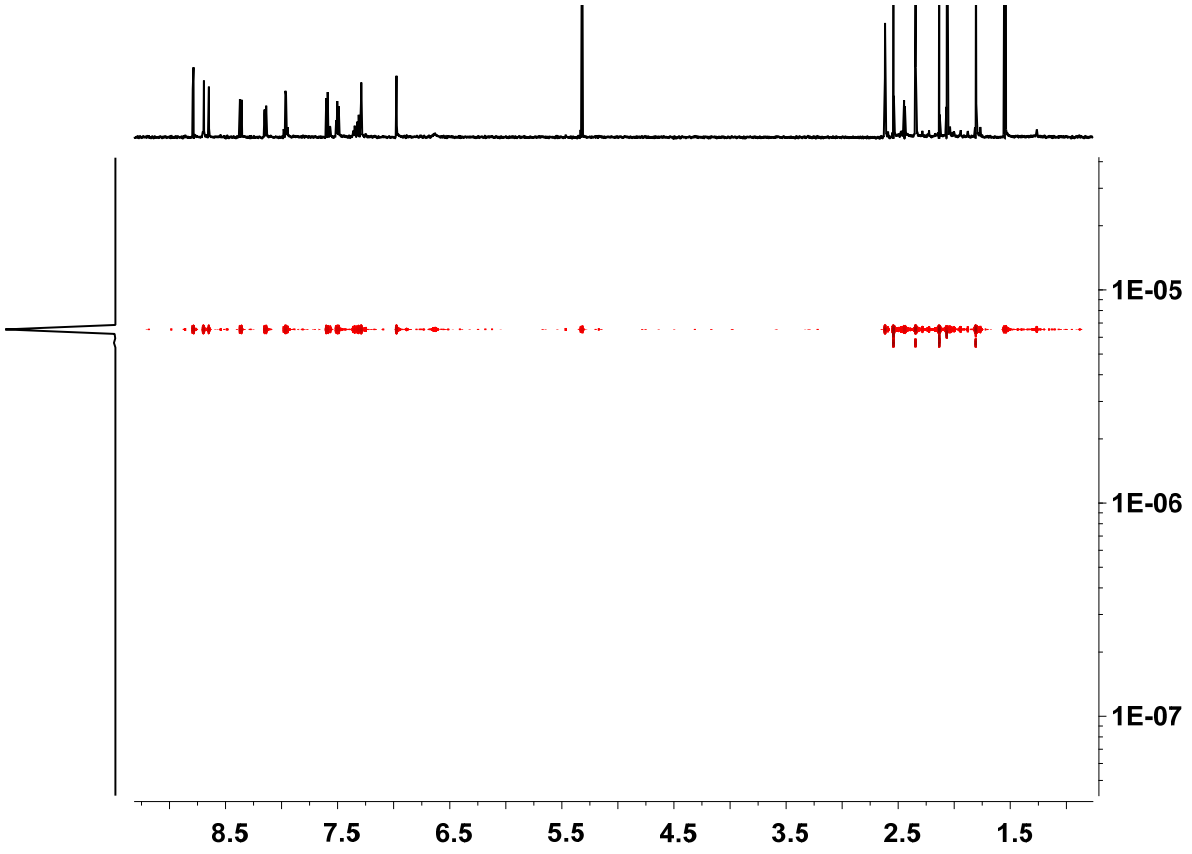

Figure S31. ^{1}H-DOSY NMR of [(**S**)•(**R**)] in CD_2Cl_2 (600 MHz, 298K). Diffusion coefficient $D = 4.3 \times 10^{-10}$ m^2 s^{-1}, Hydrodynamic radius r ~12.3 Å.

7. Variable temperature studies and determination of kinetic parameters

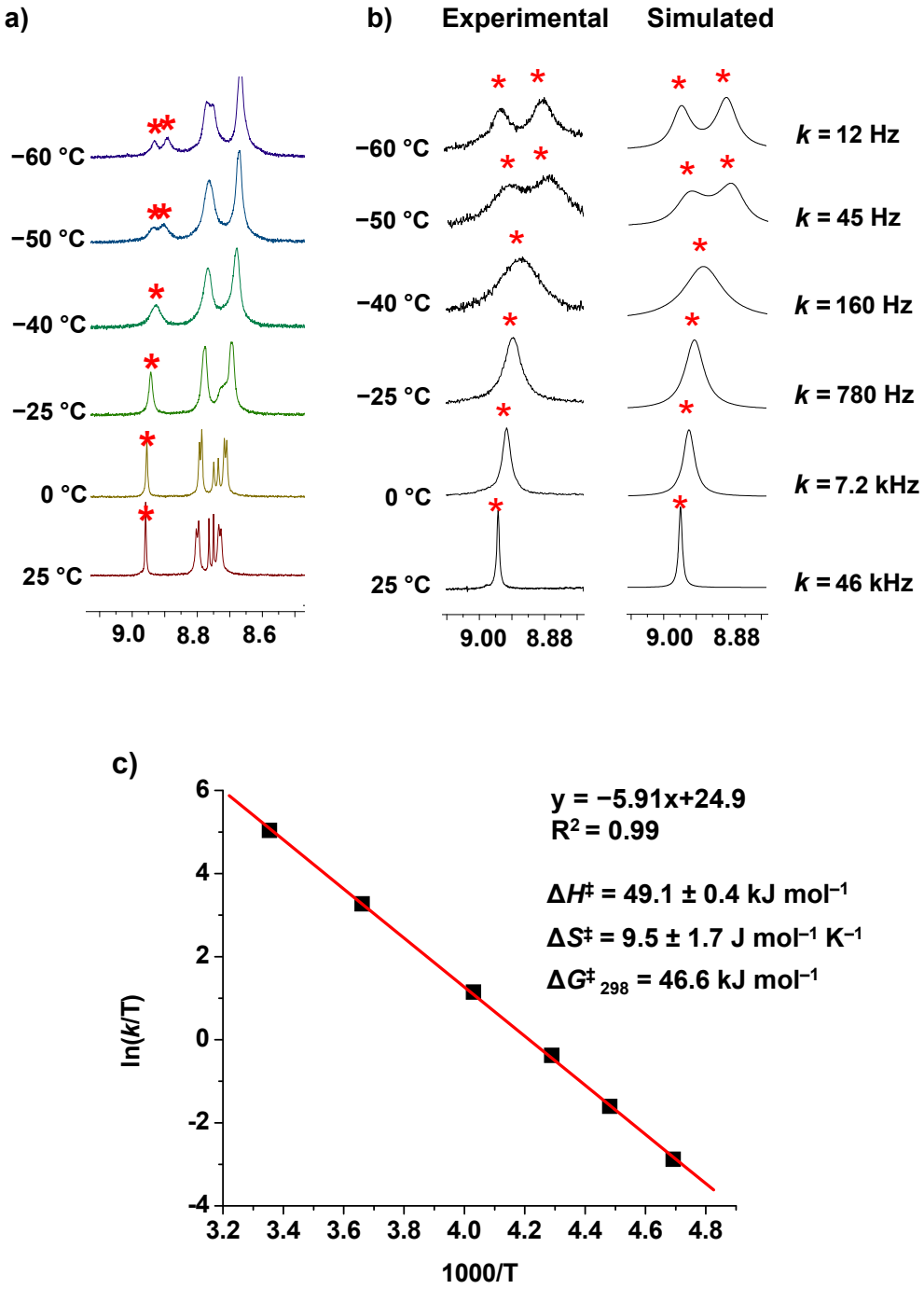

Figure S32. (a) Partial ^{1}H VT-NMR (CD_2Cl_2, 600 MHz) of $[Cu_2(\mathbf{S})(\mathbf{R})]^{2+}$ shows the splitting of proton 4′-H (red asterisk marked) in aromatic region. Upon lowering the temperature proton 4′-H splits into two sets in 1:1 ratio. (b) Experimental and theoretical splitting of proton 4′-H with exchange frequency at different temperature. (c) Eyring plot for the exchange dynamics in nanorotor $[Cu_2(\mathbf{S})(\mathbf{R})]^{2+}$.

8. ESI-MS Spectra

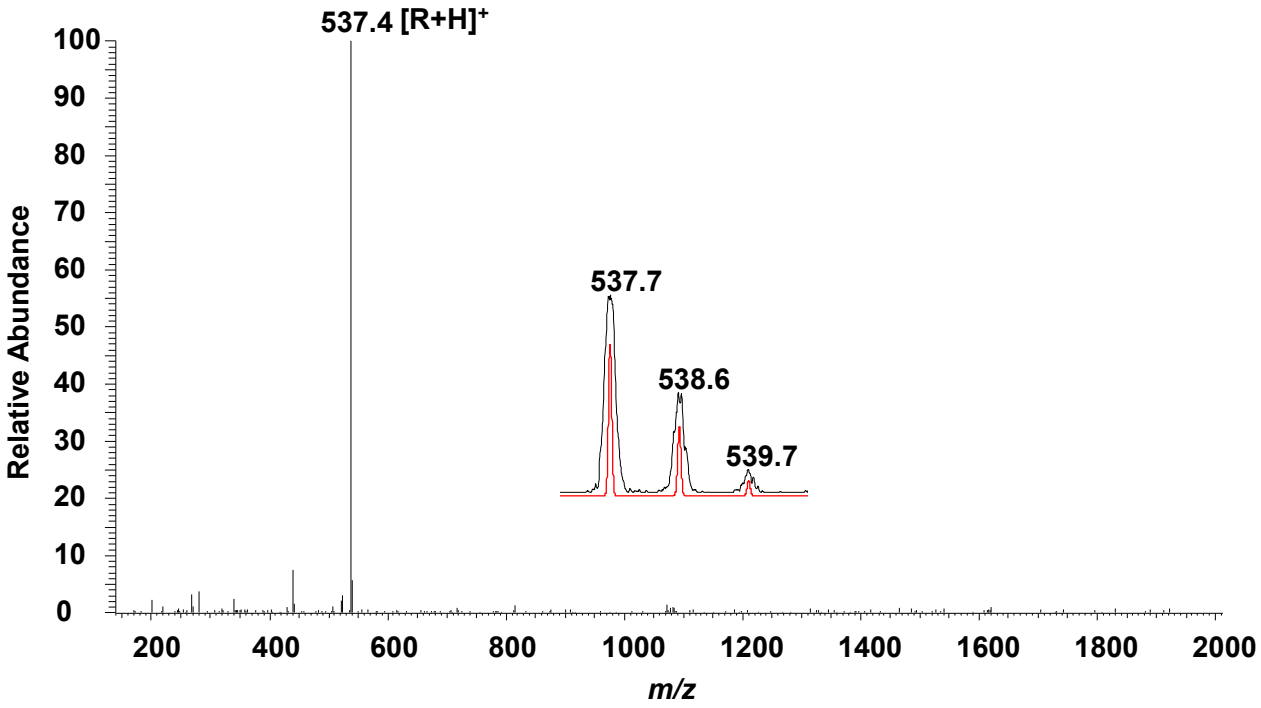

Figure S33. ESI-MS of rotator **R** after protonation.

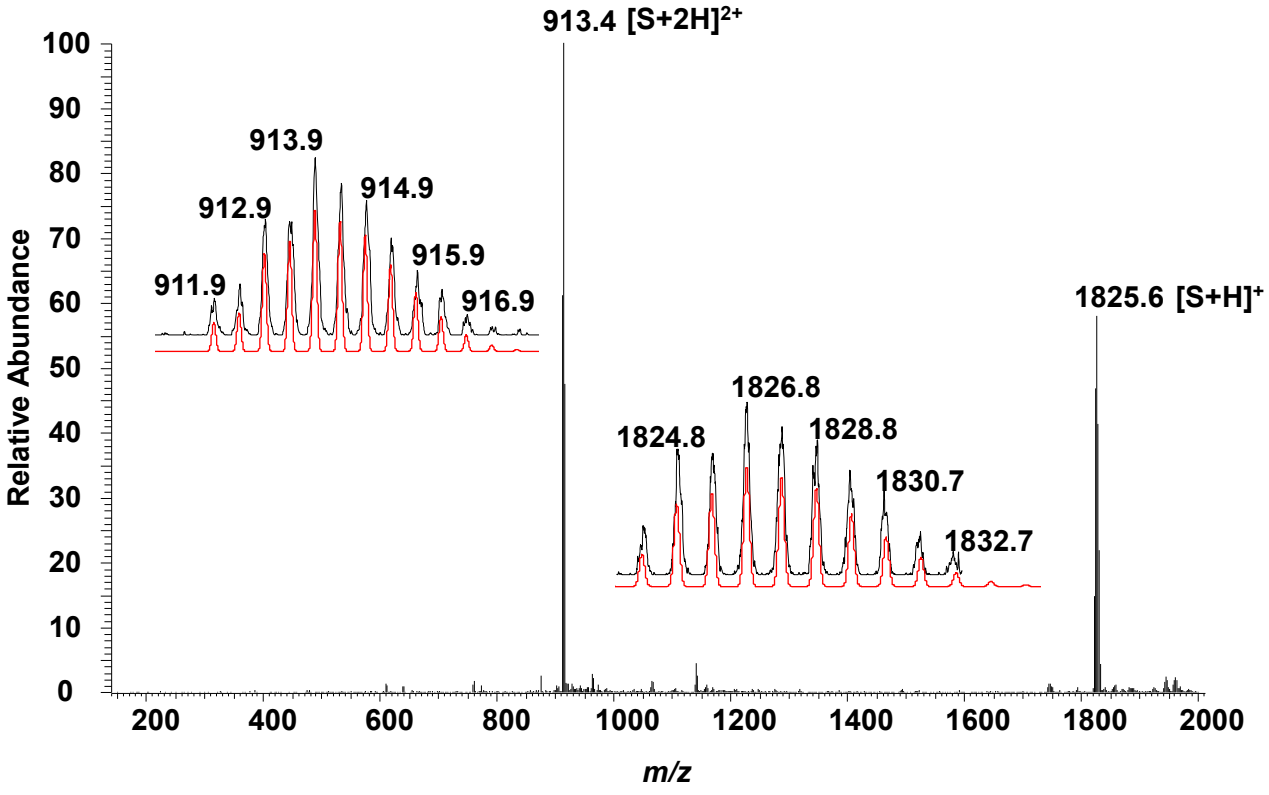

Figure S34. ESI-MS of stator **S** after protonation.

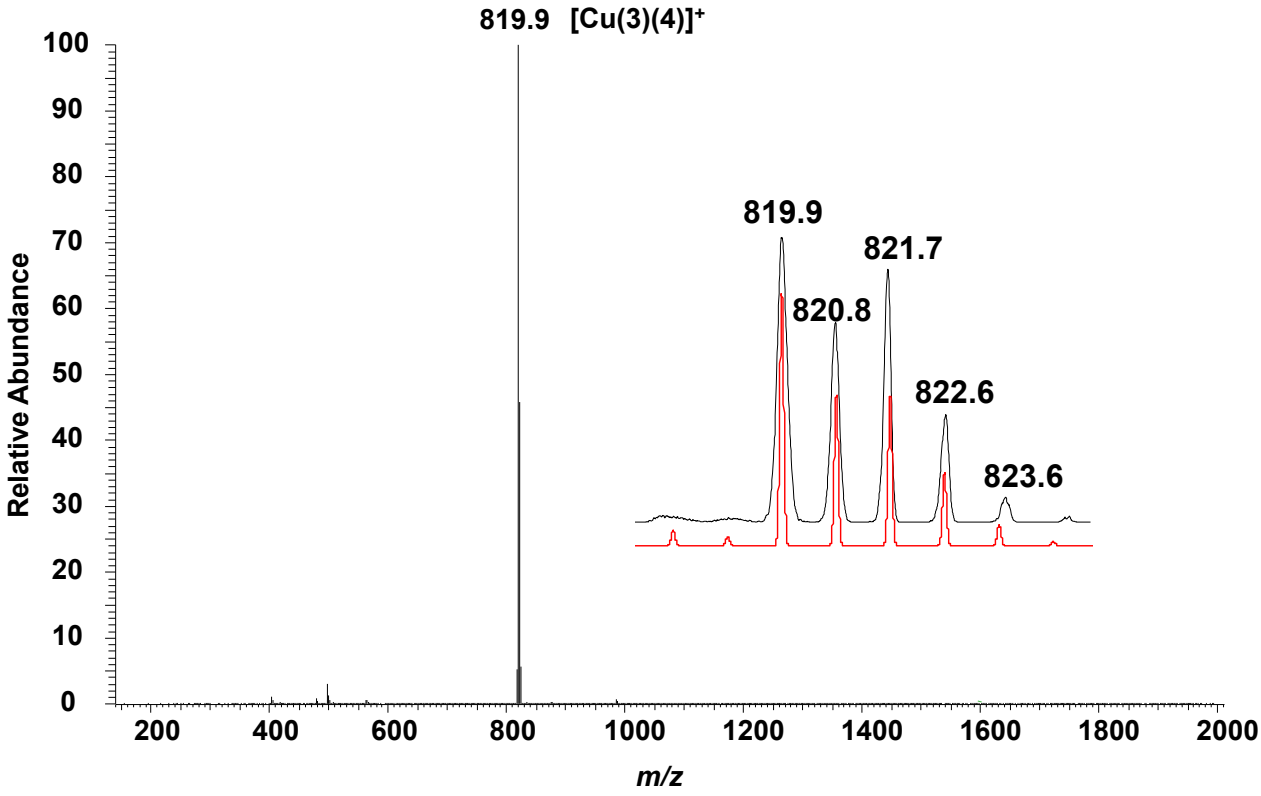

Figure S35. ESI-MS of complex **C1**.

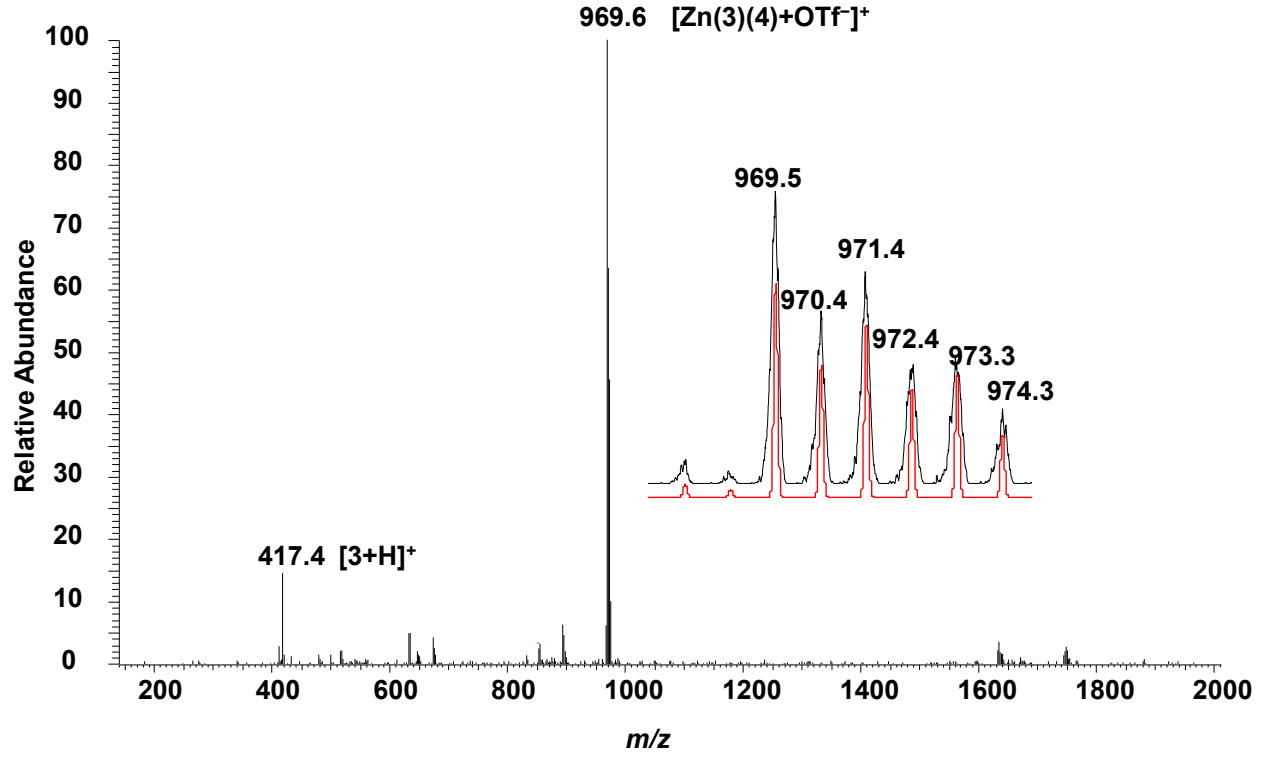

Figure S36. ESI-MS of complex **C2**.

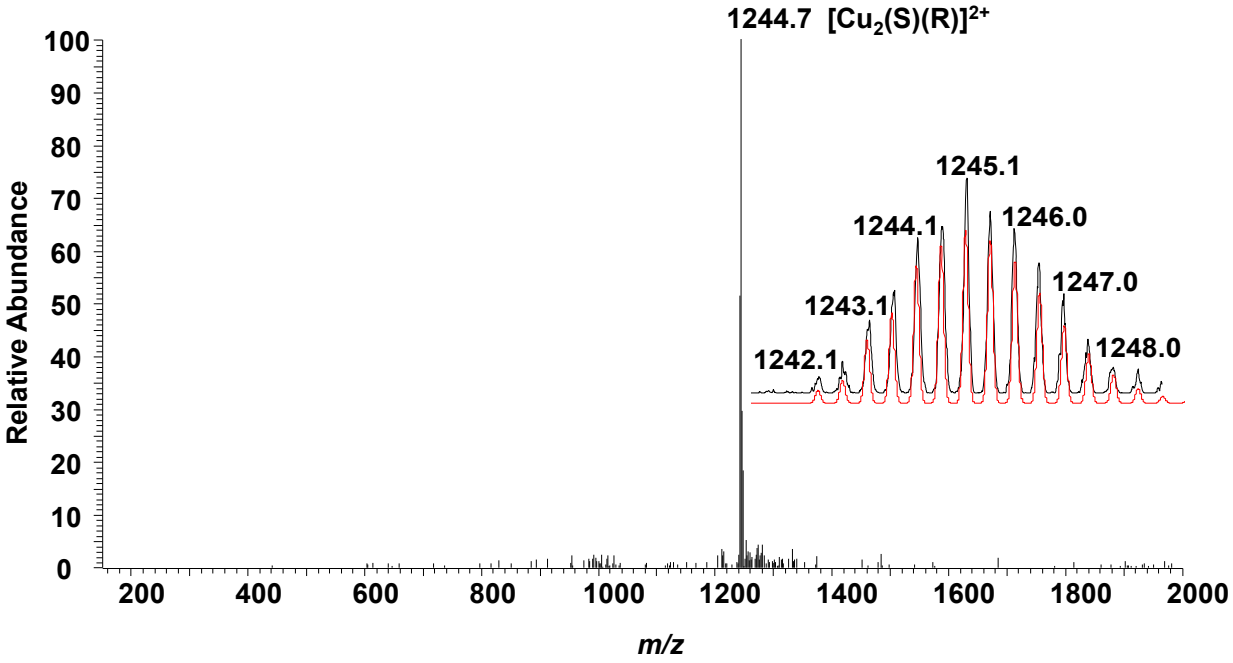

Figure S37. ESI-MS of complex **C4**.

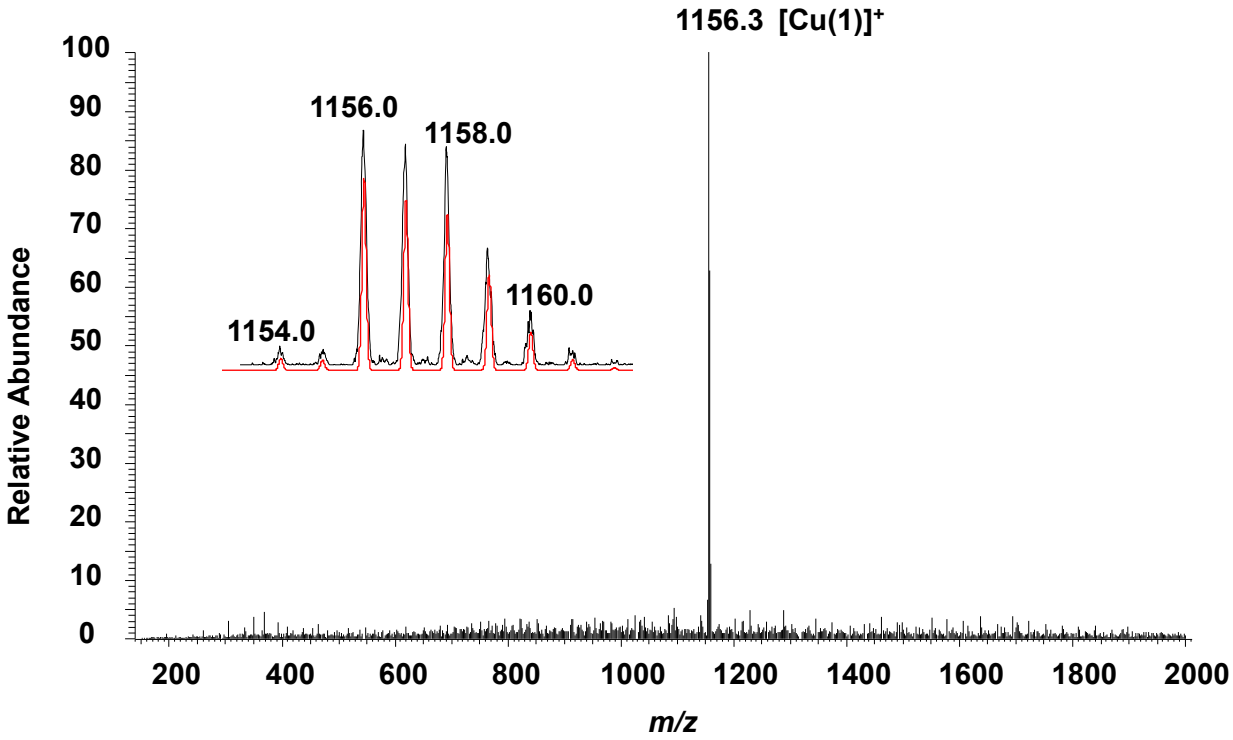

Figure S38. ESI-MS of complex **C5**.

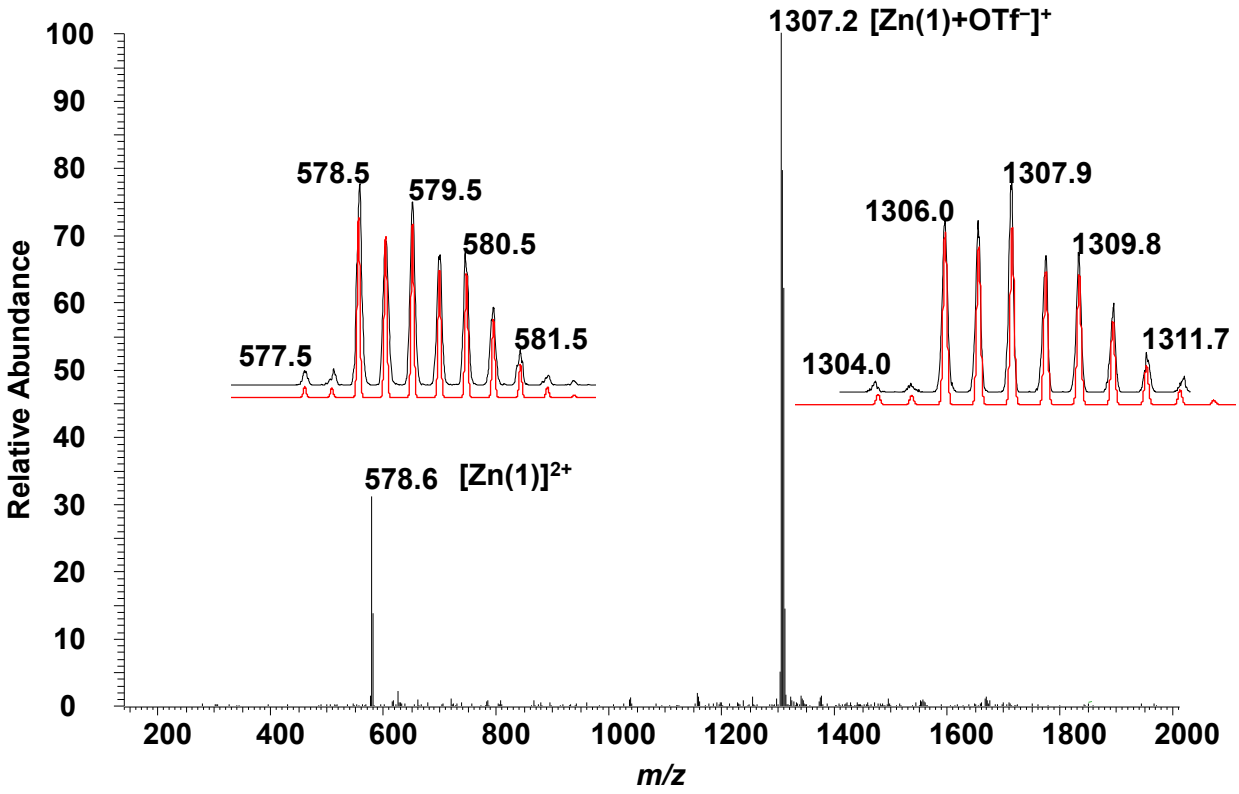

Figure S39. ESI-MS of complex **C6**.

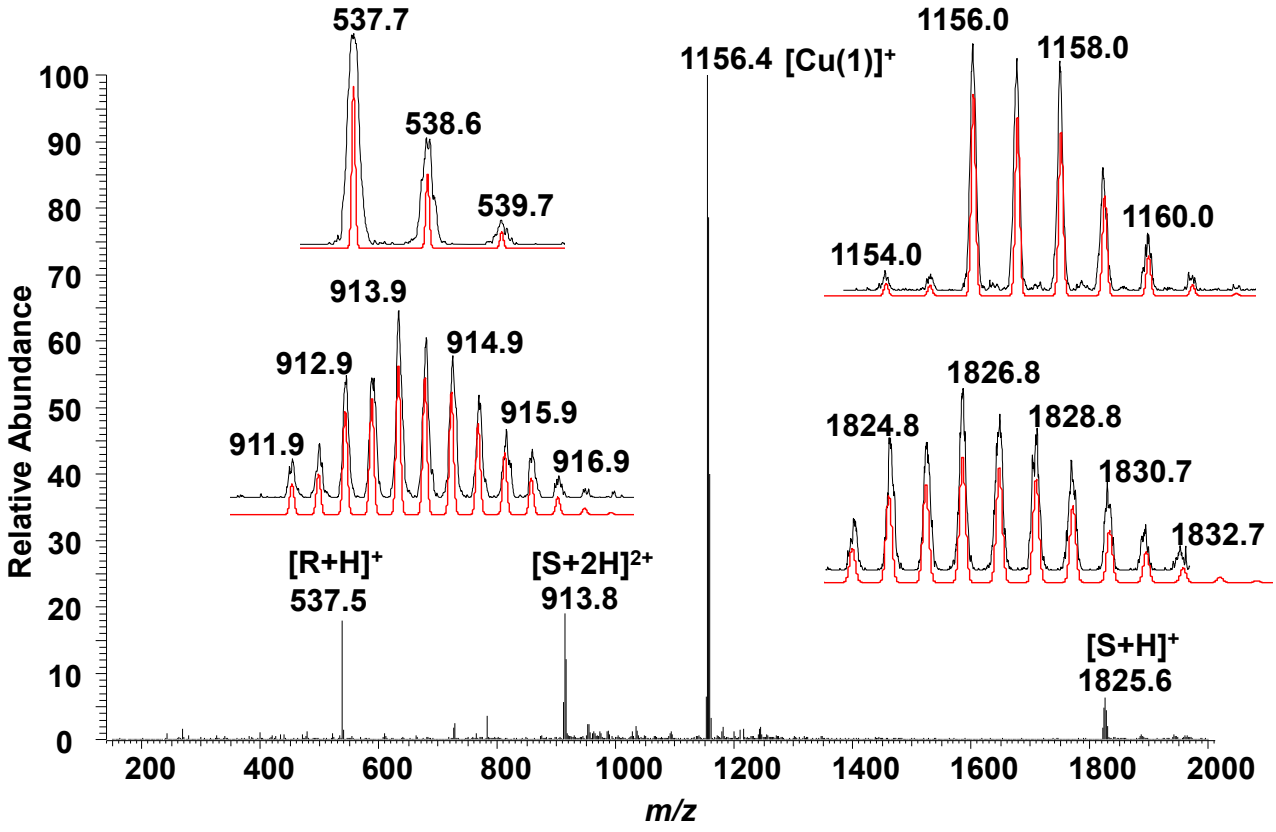

Figure S40. ESI-MS of **NetState I**.

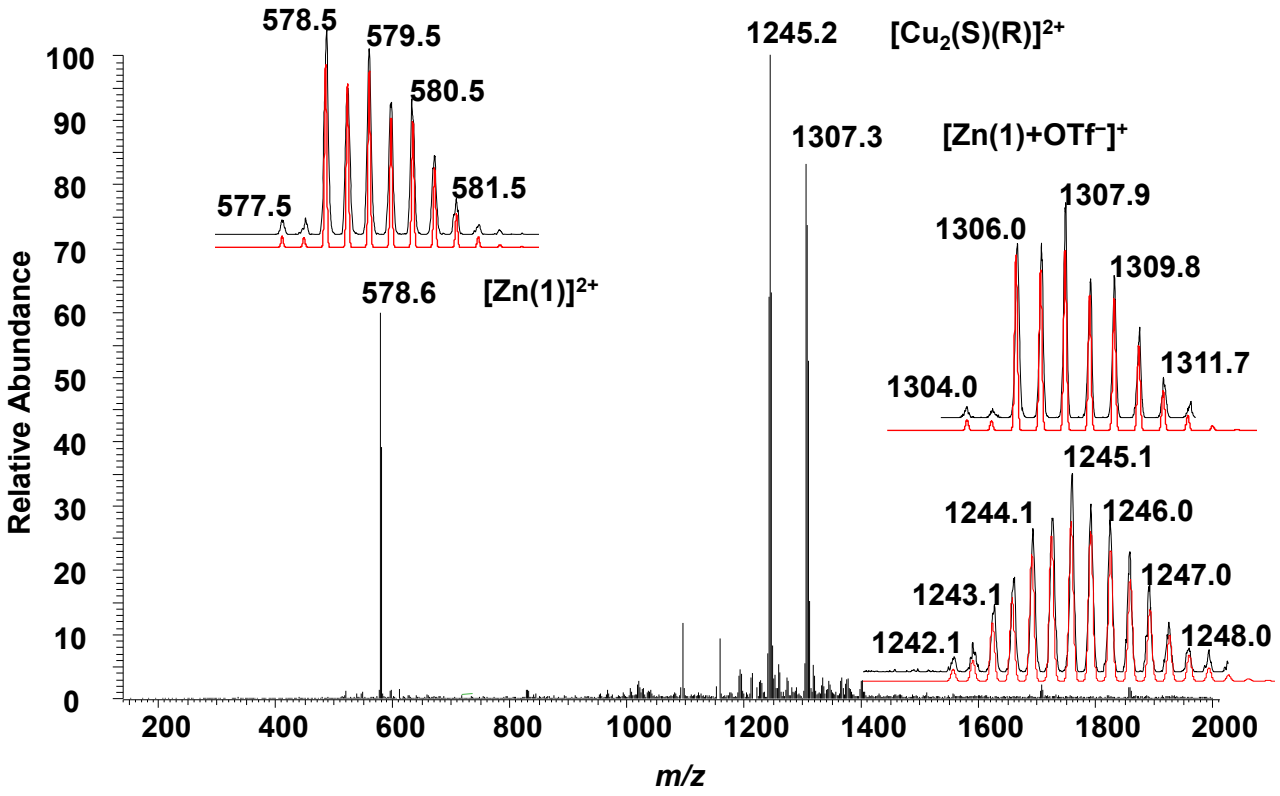

Figure S41. ESI-MS of **NetState II**.

9. UV-Vis data

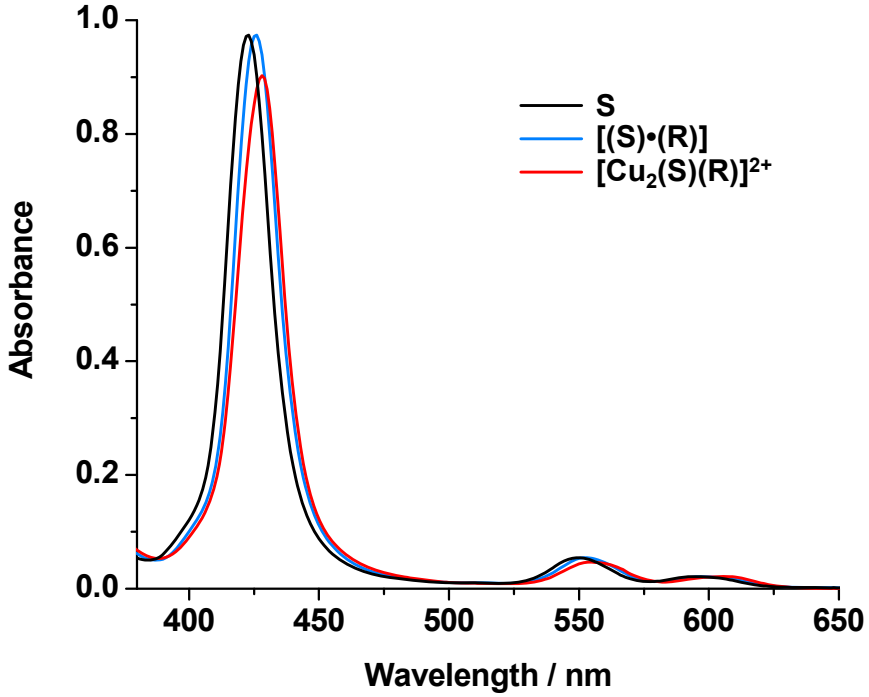

Figure S42. UV-vis spectra of stator **S**, pre-rotor [(**S**)(**R**)] and nanorotor $[Cu_2(\mathbf{S})(\mathbf{R})]^{2+}$ in CH_2Cl_2 (10^{-5} M) at 298 K.

Measurement of Binding Constant:

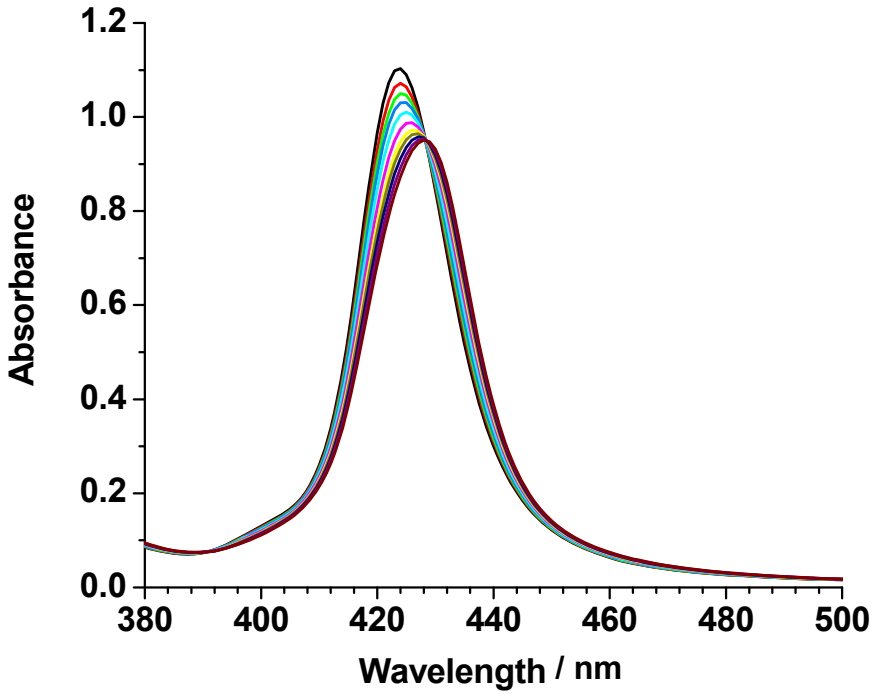

Figure S43. UV-vis titration of $[Cu_2(\mathbf{S})]^+$ (2.3×10^{-5} M) vs. **R** (1.0×10^{-3} M) in CH_2Cl_2 at 298 K. The binding constant was determined as log $K = 7.13 \pm 0.28$ using SPECFIT software.

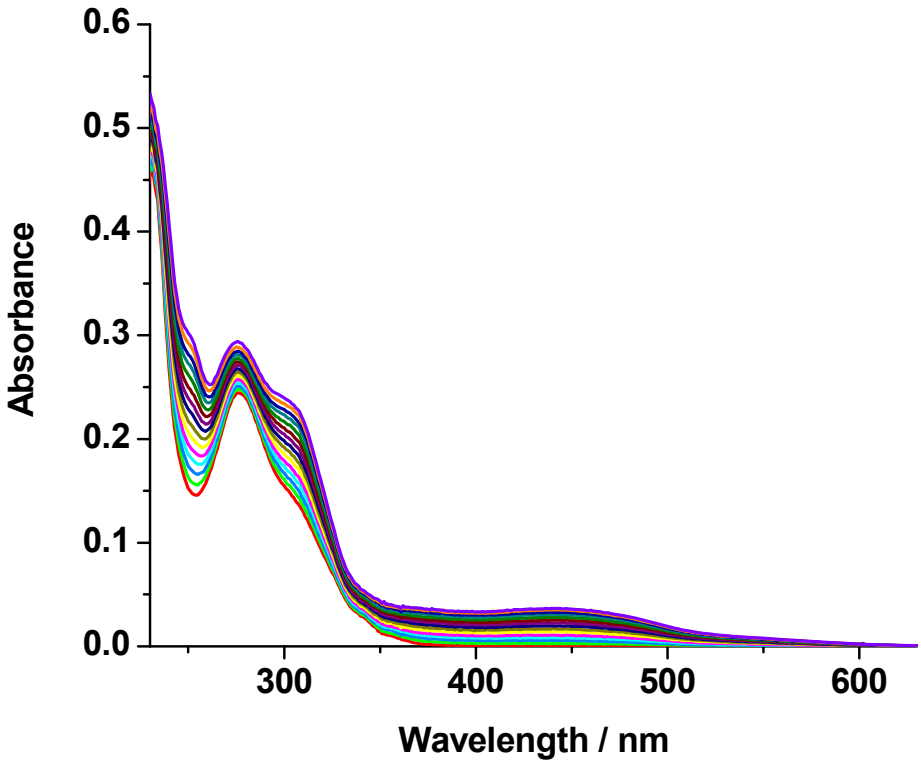

Figure S44. UV-vis titration of $[Cu(\mathbf{3})]^+$ (7.1×10^{-6} M) vs. **4** (1.4×10^{-4} M) in CH_2Cl_2 at 298 K. The binding constant was determined as log $K = 4.70 \pm 0.34$ using SPECFIT software.

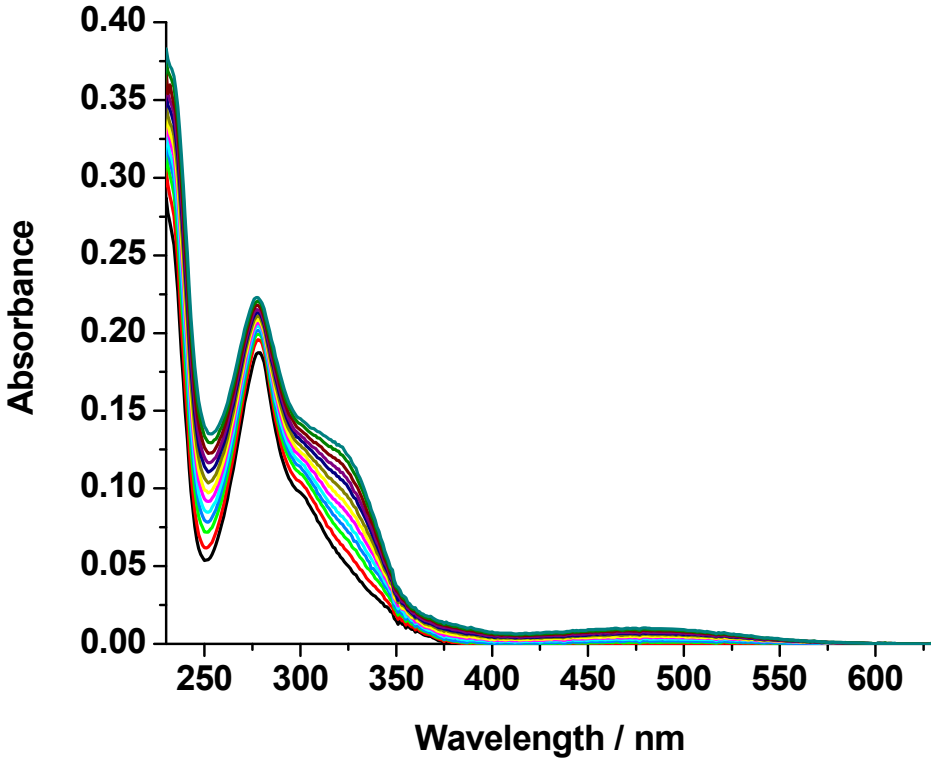

Figure S45. UV-vis titration of $[Zn(\mathbf{3})]^{2+}$ (5.6×10^{-6} M) vs. **4** (1.4×10^{-4} M) in CH_2Cl_2 at 298 K. The binding constant was determined as log $K = 7.43 \pm 0.61$ using SPECFIT software.

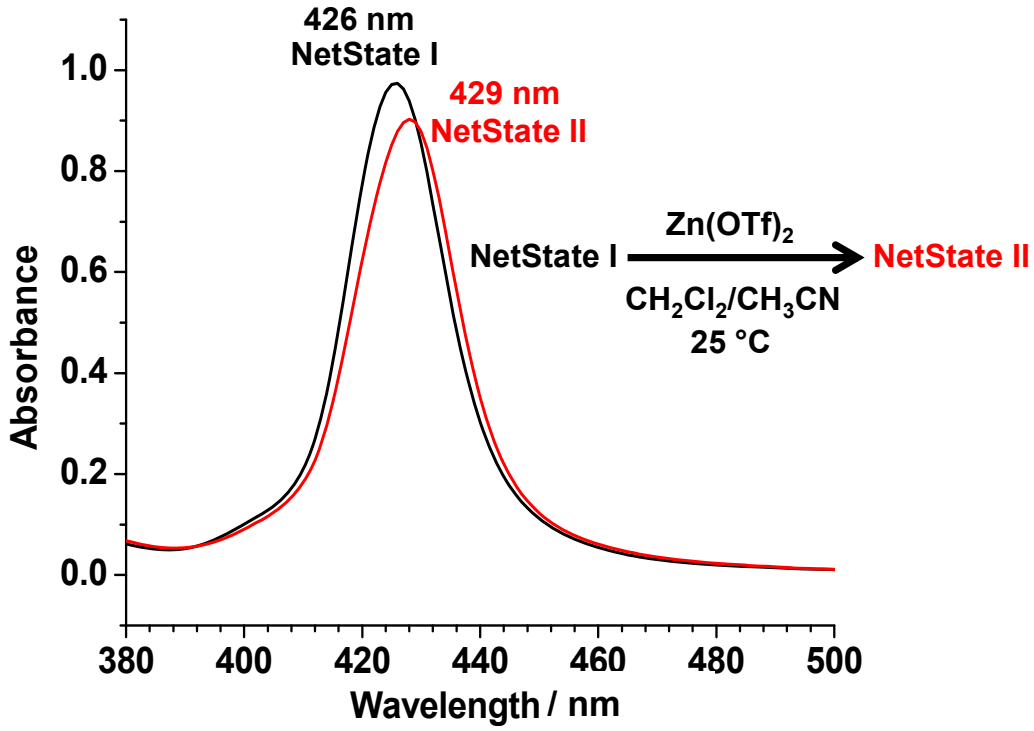

Figure S46. Change in UV-vis from **NetState I** (10^{-5} M) to **NetState II** after metal-metal exchange.

10. Speciation analysis

The binding constant of Cu^+ to the pre-rotor $[Cu(\mathbf{S})(\mathbf{R})]^+$ is log $K \sim 5.1$.[6] We derive the percentage of free copper(I) ions in solution from the speciation distribution curve. From the analysis at the given concentration, 94% of Cu^+ should be firmly bound to nanorotor $[Cu_2(\mathbf{S})(\mathbf{R})]^+$ (both used at c = 1.92 mM) and a maximum of 6% of Cu^+ is released into solution. From Figure S24 we derive that 100% of Cu^+ generate 26% yield of **AB**, thus 6% of Cu^+ may produce at most 1.6% of **AB** adding only insignificantly to the catalytic activity of the full system.

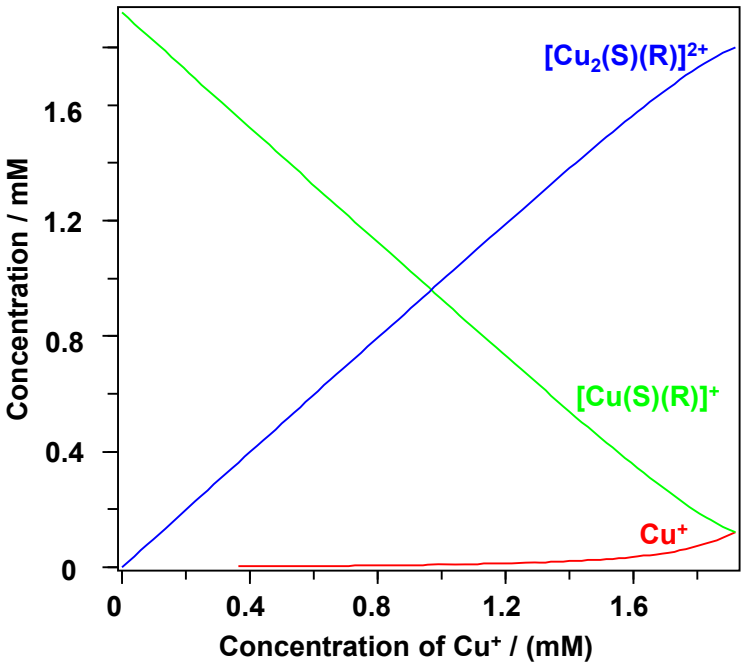

Figure S47. Calculated species distribution between $[Cu_2(\mathbf{S})(\mathbf{R})]^+$ and Cu^+ at different concentrations.

11. References

1. S. Pramanik, S. De and M. Schmittel, *Chem. Commun.,* 2014, **50**, 13254.

2. M. Schmittel, C. Michel, A. Wiegrefe and V. Kalsani, *Synthesis*, 2001, **10**, 1561.

3. A. Ambroise, R. W. Wagner, P. D. Rao, J. A. Riggs, P. Hascoat, J. R. Diers, J. Seth, R. K. Lammi, D. F. Bocian, D. Holten and J. S. Lindsey, *Chem. Mater.*, 2001, **13**, 1023.

4. S. Gaikwad, A. Goswami, S. De and M. Schmittel, *Angew. Chem., Int. Ed.*, 2016, **55**, 10512.

5. S. K. Samanta and M. Schmittel, *J. Am. Chem. Soc.*, 2013, **135**, 18794.

6. M. Schmittel, V. Kalsani, R. S. Kishore, H. Cölfen and J. W. Bats, *J. Am. Chem. Soc.*, 2005, **127**, 11544.